PNC TN951 75-15

Wear Tests of Materials for FBR in Sodium Environment (Ⅳ) Friction and Wear of Stellite No.1, Colmonoy No.6, Inconel 718, Hastelloy C, and 2¼ Cr-1Mo Steel

Mar., 1976

POWER REACTOR AND NUCLEAR FUEL DEVELOPMENT CORPORATION

PNC TN951 75-15
Mar., 1976

Wear Tests of Materials for FBR in Sodium Environment (IV) Friction and Wear of Stellite No.1, Colmonoy No.6, Inconel 718, Hastelloy C and 2¼Cr-1Mo Steel

Shigeki KANOH*,
Koichi NAKAYAMA*,
Syotaro MIZOBUCHI*,
Masaru NAMEKAWA*, and
Hideo ATSUMO*

Abstract

A series of wear tests in sodium have been carried out to develop and screen friction and wear resistant materials for sliding components of the sodium cooled reactor.

The present study was carried out on various combinations of Stellite No.1, Colmonoy No.6, Inconel 718, Hastelloy C and 2¼Cr-1Mo Steel.

The tests yielded the following results.

(1) Colmonoy No.6 was the only material that decreased in hardness after tested. The higher the temperature was, the lower became the static friction coefficient (μ_s) of Colmonoy No.6 alone.

(2) The kinetic friction coefficient (μ_k) of Stellite No.1 vs. Stellite No.1 was as high as 0.5, but it became lower (0.12) in case the mating material was Colmonoy No.6. The μ_k-value of Colmonoy No.6 vs. Colmonoy No.6 was as low as 0.2. These material combinations scarcely wore.

(3) The μ_k-value of Inconel 718 vs. Inconel 718 was as low as 0.3, but this combination wore under load more than 300 kg.

(4) The μ_k-value of Hastelloy C vs. Hastelloy C was as low as 0.23, but this combination started to wear under low load.

(5) Both the values of μ_s and μ_k of 2¼Cr-1Mo steel vs. 2¼Cr-1Mo steel were higher than 0.5, and the plastic deformation was found at the sliding surface. This combination showedthe highest wear loss of all material combinations tested.

This is the translation of the report, No.SN941 75-73, issued in Jul., 1975.

* Sodium Technology Section, Sodium Technology Division, Oarai Engineering Center.

CONTENTS

Table List

Figure List

Photo List

1. Preface

Since 1972, a series of wear and friction tests for FBR components have been carried out under the same test conditions for material selection of sliding components for FBR Up to the first half of 1974, the friction coefficients and wear rates as well as the metallographic conditions of materials in the vicinity of sliding area were determined.[1],[2],[3]

For the latter half of 1974, a series of friction and wear tests were conducted to examine and determine the friction coefficients and wear rates as well as the metallographic conditions of various material combinations of Inconel 718, Hastelloy C, Stellite No.1, Colmonoy No. 6 and $2\frac{1}{4}$Cr-1Mo steel.

2. Experimental Procedures

2-1. Test Loop

Fig. 1 shows the flowsheet of test loop. A self-welding test section (SW-2), a hot trap, a circuit of oxygen meter, and a test section for 750 °C exposure are newly attached.[4]
The soium purified by the cold trap is fed (2 - 4 ℓ/min) into the test pot (SW-1) where 3 units of test equipments (refer to Fig. 2) are installed and each unit holds one pair of test pieces as shown by Fig. 3. A detailed description for the loop is referred to the preceding report[3].

2-2. Experimental Procedures

Both the friction and wear tests were conducted entirely the same way as the preceding study[3]. The conditions of the friction and wear tests are given in Tables 1 and 2 respectively. The test conditions were constant: the sodium temperature of 450 °C (partially 280 °C), the cold trap temperature of 200 °C, the sliding contact area of 2.2 cm^2 and the sliding velocity of 3.6 cm/sec.
An incremental load is shown in Table 3. The wear test was continued for 15 minutes per each load. The total test time was 2.5 hours and the total sliding distance was 324 m.

2-3. Analytical Method

The items of analytical method were as follows:

(1) Measurement of friction coefficients.

(2) Measurement of wear rates.

(3) Measurement of sliding velocity.

(4) Measurement of surface roughness.

(5) Measurement of hardness.

(6) Observation of cross sectional microstructure (by optical microscope).

(7) Change of chemical composition by XMA.

(8) Observation by SEM.

All analyses were carried out by the same methods as those of the preceding report.[3] In addition, the total wear depth of the rotor and stator was determined from the displacement of the differential transformer attached to the end of load applying arm. The output of differential transformer was 10 mV/10 mm.

2-4. Material Combinations, Chemical Compositions, Mechanical & Physical Properties, Padding Method, and Microstructures

Tables 4, 5 and 6 show the combinations of test pieces, the chemical compositions and the mechanical and physical properties of the test specimens respectively.

Table 7 represents the coating method. All materials except Stellite No. 1 and Colmonoy No. 6 were prepared by machine work. Hastelloy C was solid solution treated. Inconel 718 was solid solution treated by oil quenching at 954 °C x 1 hr. and then machine worked. Thereafter, it was subjected to precipitation hardening treatment (719 °C x 8 hrs at the cooling velocity of 56 °C/hr and 621 °C x 8 hrs air cooled) to precipitate intermetallic compound Ni_3 (Ti, A , Nb).

Photo-1 represents the microstructures of as received test pieces. Stellite No.1 and Colmonoy No. 6 show some precipitates

Table 1 Condition of Friction Test

Na Temperature (°C)	280 and/or 450
Cold Trap Temperature (°C)	200
Apparent Contact Area of Test Piece (cm^2)	2.2
Load	Incremental Load
Quantity to be Determined	Initial Torque

Table 2 Condition of Wear Test

Na Temperature (°C)	450
Cold Trap Temperature (°C)	200
Apparent Contact Area of Test Piece (cm^2)	2.2
Sliding Velocity (cm/sec)	3.6
Load	Incremental Load
Quantity to be Determined	Sliding Torque Wear Rate

Table 3 Load, Contact Pressure and ΣPi at Each Step

Step	Load (kg)	Contact Pressure (kg/cm)	ΣPi (kg)
1	25	11.4	25
2	50	22.7	75
3	75	34.1	150
4	120	54.5	270
5	165	75.0	435
6	210	95.5	645
7	255	115.9	900
8	300	136.4	1200
9	345	156.8	1545
10	390	177.3	1935

Tested for 15 Minutes at Each Step.

of carbide. Inconel 718 indicates stratified precipitates of Ni (Ti, A , Nb) in the direction of forged elongation. The granular precipitates observed in Hastelloy C are the initially precipitated carbide M_6C and M is mainly composed of W and Mo, especially rich in Mo. Also, twins are observed.

Table 4 Material Combination

Stator	Rotor
Stellite No.1	Stellite No.1
Stellite No.1	Colmonoy No.6
Colmonoy No.6	Colmonoy No.6
Inconel 718	Inconel 718
Hastelloy C	Hastelloy C
2 1/4 Cr - 1 Mo Steel	2 1/4 Cr - 1 Mo Steel
2 1/4 Cr - 1 Mo Steel	SUS 304
2 1/4 Cr - 1 Mo Steel	Hastelloy C

Table 5 Chemical Compositions (w/o)

Material	C	Si	Ni	Co	Cr	Fe	Mn	W	Cu	Ti	Al	Mo	V	Nb Ta	P	S	B
Stellite No.1	2.58	1.16		Bal	31.33	0.28		12.49									
Colmonoy No.6	0.75	4.25	73.75		13.5	4.75											3.00
Inconel 718	0.06	0.09	52.77	0.03	18.74	Bal	0.14		0.03	1.00	0.65	3.05		4.84	0.010	0.003	0.003
Hastelloy C	0.07	0.34	Bal	T_R.	14.65	5.92	0.54	3.31				15.46	0.03		0.008	<0.005	
2 1/4Cr-1Mo Steel	0.15	0.34			2.40	Bal	0.50					1.02			0.014	0.008	
SUS 304	0.06	0.59	8.63		18.64	Bal	1.54										

Table 6 Mechanical and Physical Properties

at Room Temperature

Material	Yield Point, kg/mm²	Tensile Strength, kg/mm²	Elongation, %	Reduction of Area, %	Hardness,	Coefficient of Expansion, cm/cm/°C(×10⁻⁶)	Melting Point, °C	Specific Gravity
SUS 304	32	57	64	71	H_{RB} 76	17.3	1399∿1454	8.03
Stellite No.6	72	91	1		H_{RC} 46	13.4	1290	8.38
Stellite No.1		62	<1		H_{RC} 56	12.6	1270	8.45
Colmonoy No.6		38∿56			H_{RC} 56∿61	14.0	1040	7.85
Colmonoy No.5		40∿57			H_{RC} 45∿50	14.6	1050	8.14
Deloro Stellite SF-60M					H_{RC} 59∿62		964∿1003	7.8
Metco 16C		35∿40			H_{RC} 58∿62	14.8	1010	7.5
Inconel X750	69.4	114.8	23.6		H_{RC} 40	13.7	1330∿1430	8.3
Inconel 718	111.6	137.5	21.3	32.8	H_{RC} 43	12.8	1204∿1343	8.19
Hastelloy C	41	84	49		H_{RB} 91	13.0	1270∿1310	8.94
2 1/4Cr-1Mo Steel	45.1	59.4	30.4	76.4	H_{RB} 75	12.0		7.74
LC-1C		45.5			H_V 850			
LW-1N40		70			H_V 1050	8.5		13.2
LW-5		28			H_V 1075	8.3		10.1

Table 7 Coating Method (Substratum, SUS 304)

Coating Material	Coating Method	Coating Thickness (mm)
Stellite No.1	Oxy-Acetylene Gas Weld	2
Colmonoy No.6	Oxy-Acetylene Gas Weld	2

3. Results and Considerations.

3-1. Friction Coefficients.

3-1-1. Static Friction Coefficient μ_s.

The test piece on the rotor side was manually rotated by about 30 ° 3 times. The initial torque Ts (arithmetical mean value) was determined on a certain material combination for each load shown in Table 3. A sliding velocity was about 0.3 cm/sec and a sliding distance per one rotation was about 0.9 cm.

Fig.5 and Fig.6 show the static friction coefficient μ_s calculated from $\mu_s = T_s/(\text{Load} \times r)$ (r: mean radius of the sliding area of test piece). The values shown in Fig.5 and Fig.6 are those obtained in 280 °C and 450 °C sodium respectively.

Each combination of Inconel 718, Hastelloy C and $2\frac{1}{4}$Cr-1Mo was tested at 450 °C and not at 280 °C. All other material combinations were subjected to 280 °C test at first and then to 450 °C test. The minimum temperature of cold trap was maintained constant at 200 °C.

According to Fig. 5, all material combinations showed μ_s below 0.3 at 280 °C. Comparing μ_s under the contact pressure of 1 Kg/mm^2 the order is as follows:

$2\frac{1}{4}$Cr-1Mo vs. SUS304 ($\mu_s = 0.18$)
- Stellite No.1 vs. Stellite No.1
- Stellite No.1 vs. Colmonoy No.6 ($\mu_s = 0.22$)

$2\frac{1}{4}$Cr-1Mo vs. Hastelloy C ($\mu_s = 0.28$)

Colmonoy No.6 vs. Colmonoy No.6 ($\mu_s = 0.29$)

According to Fig. 6, μ_s has risen to about 0.8 at 450 °C. Comparing μ_s under the contact pressure of 1 Kg/mm^2, the order is as follows:

Stellite No.1 vs. Colmonoy No.6 (μ_s = 0.15)

Colmonoy No.6 vs. Colmonoy No.6 (μ_s = 0.16)

Inconel 718 vs. Inconel 718

Stellite No.1 vs. Stellite No.1 (μ_s = 0.28)

$2\frac{1}{4}$Cr-1Mo vs. SUS304 (μ_s = 0.25)

Hastelloy C vs. Hastelloy C (μ_s = 0.36)

$2\frac{1}{4}$Cr-1Mo vs. $2\frac{1}{4}$Cr-1Mo (μ_s = 0.51)

$2\frac{1}{4}$Cr-1Mo vs. Hastelloy C (μ_s = 0.78)

Fig. 7 shows μ_s under the contact pressure of 1 Kg/mm^2 in relation with material combinations and test temperatures. (kinetic friction coefficients μ_k are also shown in the same graph) The numerical values given at the right end of bar graphs represent the extent of fluctuations.

The combinations of $2\frac{1}{4}$Cr-1Mo vs. $2\frac{1}{4}$Cr-1Mo, and $2\frac{1}{4}$Cr-1Mo vs. Hastelloy C showed the most unstable behavior with μ_s fluctuations of $\pm$0.08 and $\pm$0.06 respectively (relative fluctuations, $\pm$16% and $\pm$8%). Other material combinations indicated stable friction with μ_s fluctuation within $\pm$0.03. The material combination of $2\frac{1}{4}$Cr-1Mo vs. Hastelloy C indicated an evident effect of temperature, and its μ_s rose by more than 0.6 as temperature rose. This variation indicates evidently a significant gap from the fluctuation of μ_s.

Combinations of Stellite No. 1 vs. Stellite No. 1, $2\frac{1}{4}$Cr-1Mo vs. SUS304. and $2\frac{1}{4}$Cr-1Mo vs. Hastelloy C showed increases of μ_s by 0.06, 0.075 and 0.5, respectively, with the rise of temperature. On the other hand, combinations of Colmonoy No.6 vs. Colmonoy No. 6, and Stellite No. 1 vs. Colmonoy No.6 showed decreases of μ_s by 0.12 and 0.07, respectively, with the rise of temperature.

Generally, the reduction of oxide film produced on metal surface in air will be expedited by temperature rise, and will have stronger possibility of direct contact of metals, and thus μ_s will increase. However, combinations of Colmonoy No. 6 vs. Colmonoy No. 6, and Stellite No. 1 vs. Colmonoy No. 6 showed declined values of μ_s. The reason for this phenomenon may be accounted for as follows. As shown by Table 11, most of the materials indicated increased micro-Vickers hardness on their sliding surface areas as the result of hardening effect by sliding during in-sodium friction test at 450 °C, while in the case of Colmonoy No. 6, the micro-Vickers hardness value was either the same or declined. This hardness decline of Colmonoy No. 6 was also observed at the self-welding test section.

Judging from the above, it is considerable that Colmonoy No. 6 has produced in 450 °C sodium a corrosion reaction which has caused a hardness decline. The degradated layer (or corrosion products) produced by this corrosion may reduce the value of μ_s. However, as this corrosion phenomenon is yet no more than a conjecture, it is necessary to carry out further a long term sodium exposure.

The Hastelloy C showed the highest μ_s value of 0.36 among all the hard metal alloys at 450 °C. $2\frac{1}{4}$Cr-1Mo showed higher μ_s

of 0.51 ±0.08. But when the mating material was SUS304, μ_s declined to 0.26. When the mating material was Hastelloy C, μ_s increased upto 0.78. From these findings, it is known that $2\frac{1}{4}$Cr-1Mo steel has a strong weldability.

3-1-2. Kinetic Friction Coefficient μ_k.

Kinetic friction coefficients μ_k of various material combinations were measured after the measurement of their static friction coefficients μ_s.

During rotating the rotary test piece (rotor) at 3.6 cm/sec (per mean sliding radius) under load in 450 °C sodium for 15 minutes, sliding torque T_k (mean value) was determined. Then, by increasing the load, 15-minute sliding torque T_k was determined in the similar manner. The sliding distance under each step of load was 32.4 m and the total sliding distance upto the final load of 390 Kg was 324 m (as the incremental order of load was the 10th, the total sliding time was 15 x 10 min).

The kinetic friction coefficients μ_k calculated from $\mu_k = T_k / (\text{Load} \times r)$ (r: mean sliding radius of test specimen) are shown in Fig. 10.

Comparing μ_k under the contact pressure of 1 Kg/mm^2, the order is as follows:

Stellite No.1 : Colmonoy No.6 ($\mu_k = 0.12$) < Colmonoy No.6 : Colmonoy No.6 < Hastelloy C : Hastelloy C ($\mu_k \simeq 0.22$) <

Inconel 718 ($\mu_k = 0.31$) < Stellite No.1 : Stellite No.1 < $2\frac{1}{4}$Cr-1Mo : SUS304 ($\mu_k = 0.48$) < $2\frac{1}{4}$Cr-1Mo : Hastelloy C ($\mu_k = 0.63$)

The reason for an exception of $2\frac{1}{4}$Cr-1Mo vs. $2\frac{1}{4}$Cr-1Mo combination is that as this combination showed a significant fluctuation of μ_k even under low load, its test was stopped at 120 Kg load (about 0.5 Kg/mm^2). The kinetic friction coefficient μ_k of this combination at 0.5 Kg/mm^2 was 0.57 with fluctuation of $\pm$0.29 (relative variation, $\pm$51%). Combinations with $2\frac{1}{4}$Cr-1Mo showed high μ_k values in all cases.

Combinations of hard alloy vs. hard alloy showed approximately constant μ_k against load, while combinations with $2\frac{1}{4}$Cr-1Mo showed that their μ_k rose with increasing load.

Fig. 7 shows the historiograph of μ_k for various material combinations under the contact pressure of 1 Kg/mm^2. The values given at the right end of graph represent the fluctuation of μ_k under the contact pressure of 1 Kg/mm^2. The fluctuation of μ_k for hard alloy vs. hard alloy indicated below $\pm$0.01, while combinations with $2\frac{1}{4}$Cr-1Mo steel showed μ_k fluctuations of above $\pm$0.07. The fluctuations in combinations of $2\frac{1}{4}$Cr-1Mo vs. $2\frac{1}{4}$Cr-1Mo, $2\frac{1}{4}$Cr-1Mo vs. SUS304, and $2\frac{1}{4}$Cr-1Mo vs. Hastelloy C were $\pm$0.29, $\pm$0.17 and $\pm$0.07 respectively (relative fluctuation, $\pm$51%, $\pm$35%, and $\pm$11% respectively.)

The kinetic friction coefficient μ_k of Colmonoy No.6 under the contact pressure of 1 Kg/mm^2 was the lowest among all combinations tested. Particularly, among the combinations of hard alloy vs. hard alloy, the combination of Stellite No. 1 showed the highest μ_k of 0.48, but when its mating material was Colmonoy No. 6, μ_k declined to 0.12. The reason for this is considered as sodium corrosion produced a degraded layer (or corrosion products) on Colmonoy, causing thus μ_k to decline considerably.

3-2. Wear Rate

Table 8 shows the wear depth W_d, wear volume W_v, and specific wear rate W_s obtained by scanning surface roughness tester on wear scar of stator.

The surface roughness tester was scanned on two typical scars of test specimen. W_d obtained represents the mean value of the maximum wear depth, while W_v represents the sum of the absolute values of hollowed and protruded sections from initial surface as illustrated by the following sketch (These hollowed and protruded sections were seen on $2\frac{1}{4}$Cr-1Mo steel but not on hard alloys).

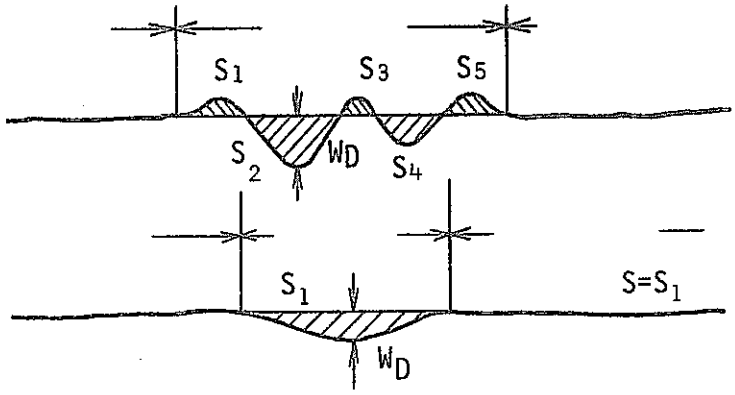

An example of $2\frac{1}{4}$Cr-1Mo steel

$S=S_1+S_2+S_3+S_4+S_5$

An example of hard alloy

W_s i.e. the wear volume per load and sliding distance was calculated by such an equation as shown in our previous report because putting incremental load during the test. That is $W_s = W_v / 900 \times V \times \Sigma Pi$. Here, V represents sliding velocity and ΣPi is shown in Table 3.

W_s of Stellite No. 1 and Colmonoy No. 6 showed the lowest value in the order of 10^{-9} mm^2/kg, while Inconel 718 and Hastelloy C showed W_s value in the order of 10^{-8} mm^2/Kg. These are about the same as W_s values shown in Table 9 obtained in our previous study.

The combination of $2\frac{1}{4}$Cr-1Mo steel, quite different from materials hitherto tested, showed extremely large W_s as 1.26×10^{-5} mm^2/Kg.

When SUS304 or Hastelloy C is taken for its mating partner, W_s is reduced by the order of two.

When W_s and W_D are plotted into logarithmic graphs, they formed approximately a linear relationship as seen at Fig. 13. Consequently, the similar evaluation of wear resistance can be made by either data.

The W_D relating to both the rotor and the stator were determined during the test (15 minutes under each load) by differential transformer and the total W_D from the beginning of test to the various load, ΣW_D, is shown in Fig. 14(A) and (B) as well as Fig. 15. Fig. 14(A) and (B) show ΣW_D obtained in the present experiment, while Fig. 15 show ΣW_D of material combinations described in the previous report.

From these diagrams, it is known that ΣW_D has increased following the increase of load. In particular, in the case of $2\frac{1}{4}$Cr-1Mo, ΣW_D shows a significant increase even under a low load (~ 120 kg). The combination of $2\frac{1}{4}$Cr-1Mo vs. SUS304 showed no wear under the load upto 165 kg but shows an sudden increase of ΣW_D (325 μm) under 210 kg. The after-test external appearance examination revealed a buckling on the rotor (both $2\frac{1}{4}$Cr-1Mo and SUS 304), which is thought to have taken place on the rotor when the above mentioned ΣW_D made a sudden increase.

When Hastelloy C is placed on the rotor side, no buckling takes place and ΣW_D variation is moderate.

Inconel X 750 among hard alloys tested shows the highest ΣW_D followed by Hastelloy C. LC-IC (B/F), LW-1N40 (B/F) and Inconel 718 indicate sudden increase of ΣW_D under the high load above 200 kg.

Combinations with SUS304 show low increase rate of ΣW_D under higher load. This is thought as the result of hardening due to plastic-work of SUS304 by sliding as shown in Table 10.

LC-IC(G/F) shows high ΣW_D even under a low load at the sliding velocity of 35.6 cm/sec.

No W_D has been detected in the combinations of Stellite No. 6 vs. Stellite No. 6, Stellite No. 1 vs. Stellite No. 1, Colmonoy No. 6 vs. Colmonoy No. 5, and Colmonoy No. 6 vs. Deloro stellite SF-60M.

3-3. Results of Metallographic Test

The following observations and measurements were undertaken in respect of sliding surface of the materials after test.

Surface roughness and hardness measurements, SEM observation and XMA surface analysis were conducted to examine the sliding surfaces. Also the sliding cross sections were subjected to optical microscopic observation to examine the changes of structure.

3-3-1. Stellite No. 1

Stellite has high hardness values and excellent wear resistance and is generally used for valve seat, pump seal ring, edge of cutters, etc.

There are many kinds of Stellite alloys, among which Stellite No. 1 is high hardness because of highly increased amount of carbide and tungsten. Its hardness excells that of Stellite No. 6, but its ductility is inferior to Stellite No. 6.

Photo-2(A) shows the cross-sectional micrographs of Stellite No. 1 paired with Stellite No. 1 after wear test.

Table 8 Wear Rate

Material Combination		Sliding Velocity, v (cm/sec)	Final Load, P (kg)	ΣP_i, (kg)	Wear Depth, W_D (μm) (Stator)	Wear Volume, W_V (mm^3) (Stator)	Specific Wear Rate, $W_S=W_V/t\times v\times \Sigma P_i$ (mm^2/kg) (Stator)
Stator	Rotor						
Stellite No.1	Stellite No.1	3.6	390	1935	∿0	∿0	∿0
Stellite No.1	Colmonoy No.6	"	"	"	0.7	0.037	5.88×10^{-10}
Colmonoy No.6	Colmonoy No.6	"	"	"	2.5	0.11	1.81×10^{-9}
Inconel 718	Inconel 718	"	"	"	13.1	1.20	1.92×10^{-8}
Hastelloy C	Hastelloy C	"	"	"	5.1	0.73	1.16×10^{-8}
2 1/4Cr-1Mo Steel	2 1/4Cr-1Mo Steel	"	120	270	251	111	1.26×10^{-5}
2 1/4Cr-1Mo Steel	SUS 304	"	390	1935	104	32.7	5.22×10^{-7}
2 1/4Cr-1Mo Steel	Hastelloy C	"	"	"	84	20.7	3.30×10^{-7}

Tested for 15 minutes at each load step.

Table 9 Wear Rate (quoted from the Preceding Report[3])

Material Combination		Sliding Velocity, v (cm/sec)	Final Load, P (kg)	ΣPi, (kg)	Wear Depth, W_D (μm) (Stator)	Wear Volume, W_V (mm^3) (Stator)	Specific Wear Rate, $W_S=W_V/t\times v\times \Sigma Pi$($mm^2/kg$) (Stator)
Stator	Rotor						
Colmonoy No.6	Deloro Stellite SF-60M	3.6(35.6)	345(390)	1545(1935)	∿0 (6)	∿0 (1.28)	∿0 (2.06×10^{-9})
Colmonoy No.5	Colmonoy No.6	3.6	390	1935	∿0	∿0	∿0
Stellite No.6	Stellite No.6	3.6	390	1935	4	0.18	2.87×10^{-9}
Inconel X750	Inconel X750	3.6	390	1935	96	30.53	4.87×10^{-7}
LC-1C(G/F)	LC-1C(G/F)	3.6(35.6)	390(120)	1935(270)	11 (86)	1.68(32.56)	2.68×10^{-8}(3.76×10^{-7})
LC-1C(B/F)	LC-1C(B/F)	3.6 (0.7)	390(390)	1935(1935)	17 (3)	3.04(0.41)	4.85×10^{-8}(3.36×10^{-8})
LW-1N40(G/F)	LW-1N40(G/F)	3.6	300	1200	6	0.13	3.34×10^{-9}
LW-1N40(B/F)	LW-1N40(B/F)	3.6	390	1935	∿0	∿0	∿0
SUS 304	SUS 304	3.6	390	1935	5	0.37	5.90×10^{-9}
SUS 304	Deloro Stellite SF-60M	3.6	390	1935	17	2.35	3.75×10^{-8}
SUS 304	Colmonoy No.6	3.6	390	1935	23	6.36	1.01×10^{-7}
SUS 304	Stellite No.6	3.6	390	1935	8	0.31	4.94×10^{-9}
SUS 304	Inconel X750	3.6	390	1935	20	1.73	2.76×10^{-8}
SUS 304	LC-1C(G/F)	3.6	390	1935	13	0.54	8.61×10^{-9}
SUS 304	LC-1C(B/F)	3.6	390	1935	10	0.99	1.58×10^{-8}
SUS 304	LW-1N40(G/F)	3.6	300	1200	35	2.74	7.04×10^{-8}

Tested for 15 minutes at each load step.

The fractured condition of carbide is observed on the surface. This is due to inferior ductility. μ_k of Stellite No. 1 was about 0.5 showing the highest value among hard alloys. This high value is thought due to the fractures of carbide. According to the previous report, Stellite No. 6 showed the μ_k of 0.3 and a stable structure.

Photo-2(B) shows the cross-sectional micrographs of Stellite No. 1 Colmonoy No. 6. Its microstructure suffered less plastic deformation and was more stable than that shown in Photo-2(A). μ_k was extremely low, 0.12. It showed an excellent wear resistance with no W_D detected.

3-3-2. Colmonoy No. 6

Photo-3 shows the cross-sectional micrographs of Colmonoy No. 6 after wear test. Photo-3(A) is in the case when the mating material was Colmonoy No. 6, and (B) is in the case when the mating material was Stellite No. 1. The dark spots seen in Photo-3(B) represent the blowholes made and remained during coating process of Colmonoy No. 6. The cracks seen at the edge of structure are thought due to the effect of the configuration of test specimen. Therefore, appropriate caution must be taken for the configuration of the part where coating is applied.

Despite the fracture appearing on the sliding face, μ_s and μ_k of Colmonoy No. 6 were 0.16 and 0.21 respectively, and μ_s and μ_k of Colmonoy No. 6 paired with Stellite No. 1 were 0.15 and 0.12 respectively. These values are extremely low comparing with those of other materials. As the reason for this, some reaction of Colmonoy No. 6 with sodium is considered. Though Colmonoy No. 6 is hard, brittle and easy to crack, it is expected

to demonstrate excellent wear resistance when appropriate caution is paid for coating configuration.

3-3-3. Inconel 718

Inconel 718 is a type of precipitation hardening alloy, such as Inconel X 750 described in our previous report[3], by adding Ti, Aℓ, Nb and age-treated to precipitate intermetallic compound Ni_3 (Ti, Aℓ, Nb) which increases high temperature strength.

It is extremely strengthened comparing with other materials, and is applied for the parts of jet engines and gas turbines.

Photo-4 shows the cross-sectional micrographs of before and after wear test. The fine dark spots scattered in austenite structure are considered as the precipitated Ni_3 (Ti, Aℓ, Nb). There is seen a plastic deformation in the vicinity of the sliding cross section.

As shown by Fig. 14(A), the wear of Inconel 718 increased abruptly (about 70 μm) at the load of 300 kg, while no wear was detected under lower load. It is considered that this abrupt increase is due to the rise of temperature of friction surface upto the level to turn the precipitates into solid solution. However, μ_k was constant at about 0.3 upto the high load.

3-3-4. Hastelloy C

Photo-5 shows the cross-sectional micrographs of Hastelloy C after wear test. Both combinations with Hastelloy C and $2\frac{1}{4}$Cr-1Mo showed the traces of plastic deformation in the vicinity of the sliding surface of Hastelloy C.

Photo-6 shows the results of XMA surface analysis of Hastelloy C paired with $2\frac{1}{4}$Cr-1Mo. There was observed a

maldistribution of Fe and Ni. This is because of the adhesion of $2\frac{1}{4}$Cr-1Mo on Hastelloy C.

Photo-7 represents the SEM photographs showing the rough surface because of the adhesion of $2\frac{1}{4}$Cr-1Mo.

μ_k of Hastelloy C vs. Hastelloy C was a low value of about 0.2, while that paired with $2\frac{1}{4}$Cr-1Mo was high with about 0.6 showing unstability.

3-3-5. $2\frac{1}{4}$Cr-1Mo Steel

$2\frac{1}{4}$Cr-1Mo steel is used for heat transfer tubes of FBR steam generator. There have been issued various reports[5]-[7] on creep characteristics and transfer phenomena of constituting elements. However, there has been undertaken no experiment relating to problems arising from vibration and sliding between heat transfer tubes and their supports caused by sodium flow and temperature change.

In particular, as a heat transfer tube involves a possibility of sodium-water reaction, it is absolutely necessary to secure safety by investigating the mechanism and phenomena of friction, wear and fretting of support section.

$2\frac{1}{4}$Cr-1Mo has lower strength (tensile strength 59.4 kg/mm^2) than ordinary friction-resistant and wear-resistant materials and is susceptible to plastic deformation. Therefore, it is expected this is inferior in friction resistance and wear resistance.

As shown in Fig. 10, $2\frac{1}{4}$Cr-1Mo indicated μ_k more than 0.5.

Also as shown in Fig. 14, $2\frac{1}{4}$Cr-1Mo indicated the most significant wear rate among all materials tested. Photo-8 shows the cross-sectional micrographs of $2\frac{1}{4}$Cr-1Mo steel. In the case of the homogeneous combination of $2\frac{1}{4}$Cr-1Mo, the plastic deformed

layer was observed to the depth of 150 μm. When the partner material was SUS304, there was observed transfer of SUS304 onto the sliding surface of $2\frac{1}{4}$Cr-1Mo. When the partner material was Hastelloy C, any transfer of Hastelloy C was not observed onto the sliding surface of $2\frac{1}{4}$Cr-1Mo. Both photographs show quite significant roughness of sliding surface.

Photo-9 shows the cross-sectional micrographs of SUS304 paired with $2\frac{1}{4}$Cr-1Mo. There is observed a plastic deformation in the vicinity of the sliding surface of SUS304. It is noticed the configuration of test piece before and after test has changed considerably, and also there is noticed adhesion of $2\frac{1}{4}$Cr-1Mo onto SUS304.

Photo-10 represents SEM photographs of $2\frac{1}{4}$Cr-1Mo surface before and after test. Obvious plastic flows and adhesion of wear debris are observed on the surface after test.

Photo-11 shows the sliding surface of SUS304 paired with $2\frac{1}{4}$Cr-1Mo after test. This corresponds to Photo-10(C) showing quite similar surface each other.

Its surface condition was quite rough and indicated cohesion of abrasion particles.

Photo-12 and 13 show the results of XMA surface analysis performed to examine the adhesion of partner material.

$2\frac{1}{4}$Cr-1Mo steel paired with SUS304 showed the differences in Ni and Cr concentrations in places on sliding surface and sliding cross section. The adhesion of partner material SUS304 was observed in areas where concentration of Ni and Cr was high, while on the surface of SUS304 there took place adhesion of partner material $2\frac{1}{4}$Cr-1Mo in areas where concentration of Ni and Cr was

low. This is also obvious from the cross-sectional micrographs shown in Photo-8 and 9.

3-3-6. Hardness Measurement

Tables 10 and 11 show the hardness determined vertically to the sliding surface of test piece before and after test. The values given in Table 10 are those of material combinations described in the previous report. The values given in Table 11 represent those of material combinations in the present study. Almost all the materials showed increased hardness values after test. Especially both SUS304 and $2\frac{1}{4}$Cr-1Mo showed about 2-fold increase of microhardness. $2\frac{1}{4}$Cr-1Mo paired with SUS304 showed as much as 3-fold increase of microhardness value due to adhesion of SUS304.

On the other hand, LW-5 and Colmonoy No. 6 showed a decline of microhardness. LW-5 suffered a bulk deformation of coating layer during the test and its hardness decline was thought due to the breakaway of intergrain bonding. Colmonoy No. 6 showed a hardness decline by about Hv 200 when mating material was Colmonoy No. 5 or No. 6. Colmonoy No. 6 showed a hardness decline even in non-sliding area after sodium exposure (no hardness decline was observed in respect of other materials). This hardness decline is thought due to certain reaction (corrosion, decarburization, etc.) of sodium with Colmonoy No. 6.

The hardness increase of material surface by plastic work is considered to reduce wear according to Holm's law.

Holm's law $$W = k \cdot \frac{P \times \ell}{Pm}$$

k: Constant

P: Load

ℓ: Sliding distance

Pm: Indentation hardness

3-3-7. Surface Roughness Measurement

Table 12 shows the surface roughness of materials before and after test. Combinations of hard alloys hardly show any change of surface roughness. Inconel 718 showed the largest change among these materials.

$2\frac{1}{4}$Cr-1Mo showed considerable surface roughness after test. $2\frac{1}{4}$Cr-1Mo homogeneous combination showed much larger surface roughness as high as 52 μm. When partner material was a harder material, surface roughness of $2\frac{1}{4}$Cr-1Mo declined: 36 μm and 15 μm in the case paired with SUS304 and Hastelloy C respectively.

Table 10 Microhardness of Materials Described in the Preceding Report[2],[3] (Hv)

100g

Material Determined	Mating Material	Microhardness (Hv)	
		as Received	after Tested
Deloro Stellite SF-60M	Colmonoy No.6	762	894
Colmonoy No.5	Colmonoy No.6	464	657
Colmonoy No.6	Colmonoy No.5	824	592
Stellite No.6	Stellite No.6	585	907
Inconel X750	Inconel X750	459	592
LC-1C (G/F)	LC-1C (G/F)	782	1033
LW-1N40(G/F)	LW-1N40(G/F)	1267	1427
SUS 304	SUS 304	298	639
SUS 304	Colmonoy No.6	298	624
SUS 304	Stellite No.6	298	579
Stellite No.6	SUS 304	585	752
SUS 304	Stellite No.1	298	457
SUS 304	Inconel X750	298	554
SUS 304	LC-1C (G/F)	298	649
SUS 304	LW-1N40(G/F)	298	613
SUS 304	LW-5	298	606
LW-5	SUS 304	1097	579

Determined vertically to the sliding surface.

Table 11 Microhardness of Materials Described in the Present Report (Hv)

100g

Material Determined	Mating Material	Microhardness (Hv)		
		as Received	after Tested	
			Non-Sliding Surface	Sliding Surface
Stellite No.1	Stellite No.1	870 1650*		914
Stellite No.1	Colmonoy No.6	870 1650*	804	1035
Colmonoy No.6	Stellite No.1	824 1854*		835
Colmonoy No.6	Colmonoy No.6	824 1854*	659	615
Inconel 718	Inconel 718	503	563	583
Hastelloy C	Hastelloy C	429	442	714
2 1/4Cr-1Mo Steel	2 1/4Cr-1Mo Steel	232	223	456
2 1/4Cr-1Mo Steel	SUS 304	232	239	660
2 1/4Cr-1Mo Steel	Hastelloy C	232	256	642
SUS 304	2 1/4Cr-1Mo Steel	298		479
Hastelloy C	2 1/4Cr-1Mo Steel	429		627

* Hardness of Carbide Precipitated

Determined Vertically to the Sliding Surface

Table 12 Roughness

Material Combination		Roughness (μm)				Sliding Velocity (cm/sec)	Final Load (kg)
Stator	Rotor	As Received		After Tested			
		Stator	Rotor	Stator	Rotor		
Stellite No.1	Stellite No.1	0.4	0.4		0.6	3.6	390
Stellite No.1	Colmonoy No.6	0.4	1	0.7	1	3.6	390
Colmonoy No.6	Colmonoy No.6	1	1	1	2	3.6	390
Inconel 718	Inconel 718	0.7	0.7	7	2	3.6	390
Hastelloy C	Hastelloy C	2	2	2	3	3.6	390
2 1/4Cr-1Mo Steel	2 1/4Cr-1Mo Steel	2	2	52	19	3.6	390
2 1/4Cr-1Mo Steel	SUS 304	2	0.4	36	4	3.6	390
2 1/4Cr-1Mo Steel	Hastelloy C	2	2	15	5	3.6	390

4. Conclusion

The results of present friction and wear tests are as follows:

(1) Colmonoy No. 6 alone showed hardness decline after the test, and also indicated decline of static friction coefficient (μ_s) as temperature rose.

(2) Stellite No. 1 in homogeneous combination showed relatively high μ_k value about 0.5. But with Colmonoy No. 6 as its partner material, μ_k declined to 0.12. Colmonoy No. 6 in homogeneous combination showed low μ_k at 0.2. Hardly any wear was observed on these materials.

(3) Inconel 718 in homogeneous combination indicated low μ_k at 0.3, and under the load above 300 kg, it began to indicate initiation of wear (W_D was 70 μm under 300 kg).

(4) Hastelloy C in homogeneous combination indicated low μ_k at 0.23, while it showed initiation of wear from the low load region.

(5) $2\frac{1}{4}$Cr-1Mo in homogeneous combination showed high μ_s and μ_k above 0.5 for both, and it indicated conspicuous plastic deformation in the sliding area. It presented the highest wear rate among all the tested materials. When its partner material was either SUS304 or Hastelloy C, its W_D declined.

5. Bibliography

(1) Shigeki Kanoh, Shotaro Mizobuchi, et al.: "Wear Tests of Materials for FBR in Sodium Environment (I), Wear of Hard Alloys," SN941 73-17.

(2) Shigeki Kanoh, Shotaro Mizobuchi, et al.: "Wear Tests of Materials for FBR in Sodium Environment (II), Friction and Wear of Hard Alloys and Carbides," SN941 74-12.

(3) Shigeki Kanoh, Shotaro Mizobuchi, et al.: "Wear Tests of Materials for FBR in Sodium Environment (III), Metallographic Test on Hard Alloys and Carbides," SN941 74-80.

(4) Syotaro Mizobuchi, Shigeki Kanoh, et al.: "Self-Welding Test in High Temperature Sodium (IV), and Trial Manufacture and Performance Test on New Model of Self-Weld Test Machine," SN941 75-13.

(5) Shun-ichi Yuhara, et al.: "Creep Characteristics of $2\frac{1}{4}$Cr-1Mo for FBR in High Temperature Sodium." N941 74-62.

(6) Akira Maruyama, et al.: "In-Sodium Mass Transfer Test on $2\frac{1}{4}$Cr-1Mo for FBR Structural Material (I), and Results of 1,000 Hr Continuous Dipping Test by Material Test Loop." SN941 72-03.

(7) Akira Maruyama, et al.: "In-Sodium Mass Transfer Test on $2\frac{1}{4}$Cr-1Mo for FBR Structural Material (II), and Results of 2,000 Hr Continuous Dipping Test." SN941 73-14.

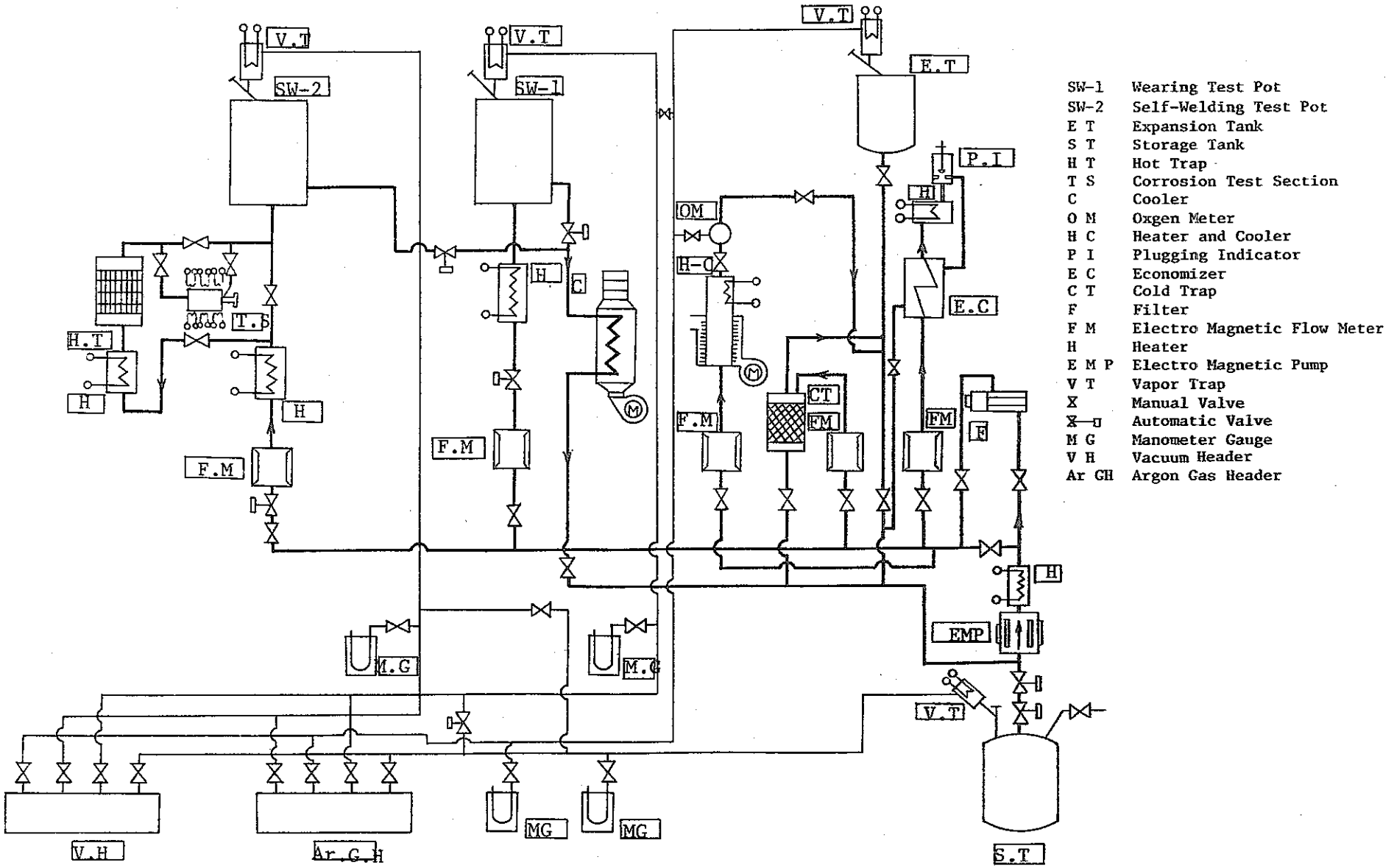

Fig. 1 Self-Welding and Wearing Test Loop Flow Sheet

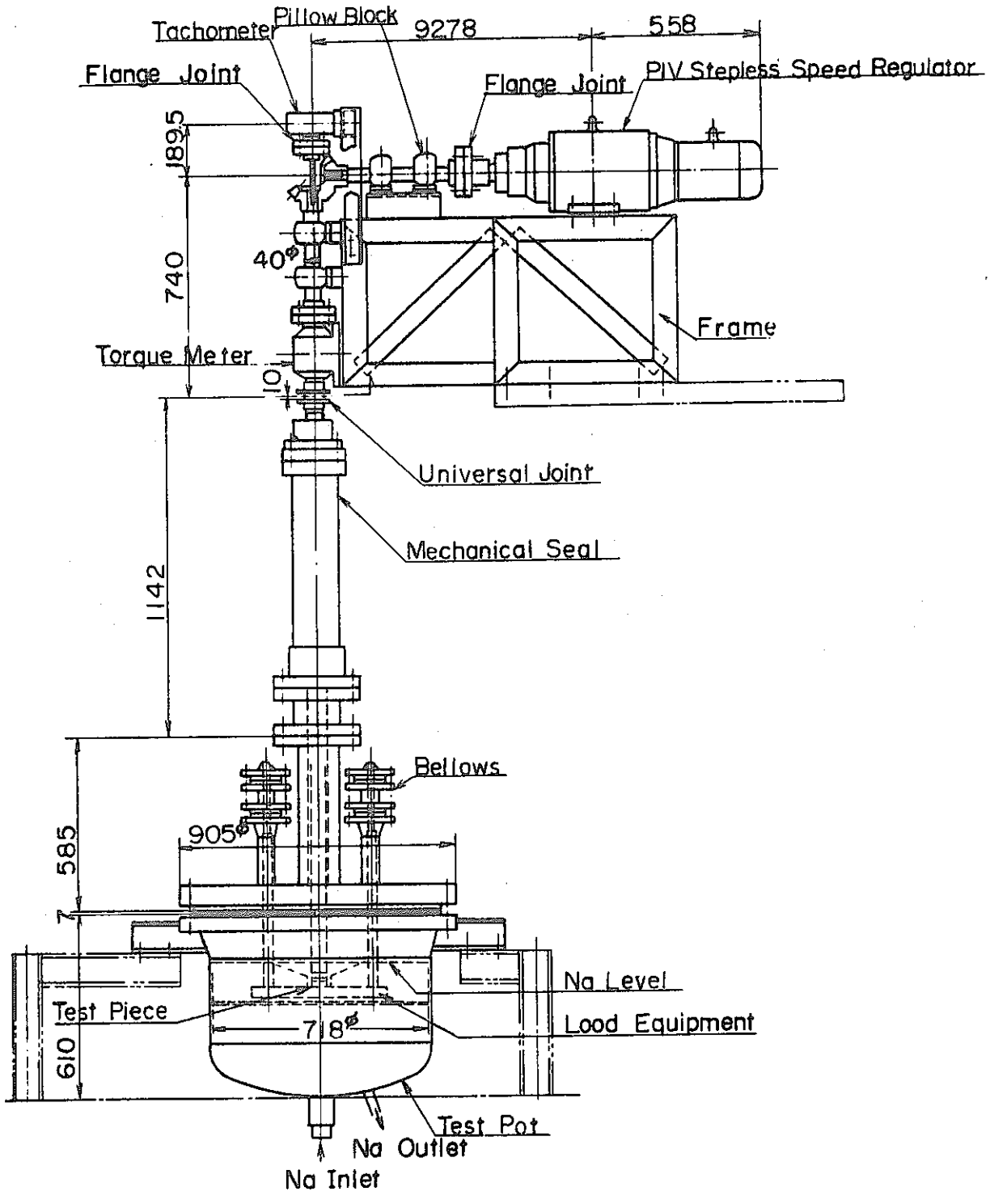

Fig. 2 Test Equipment

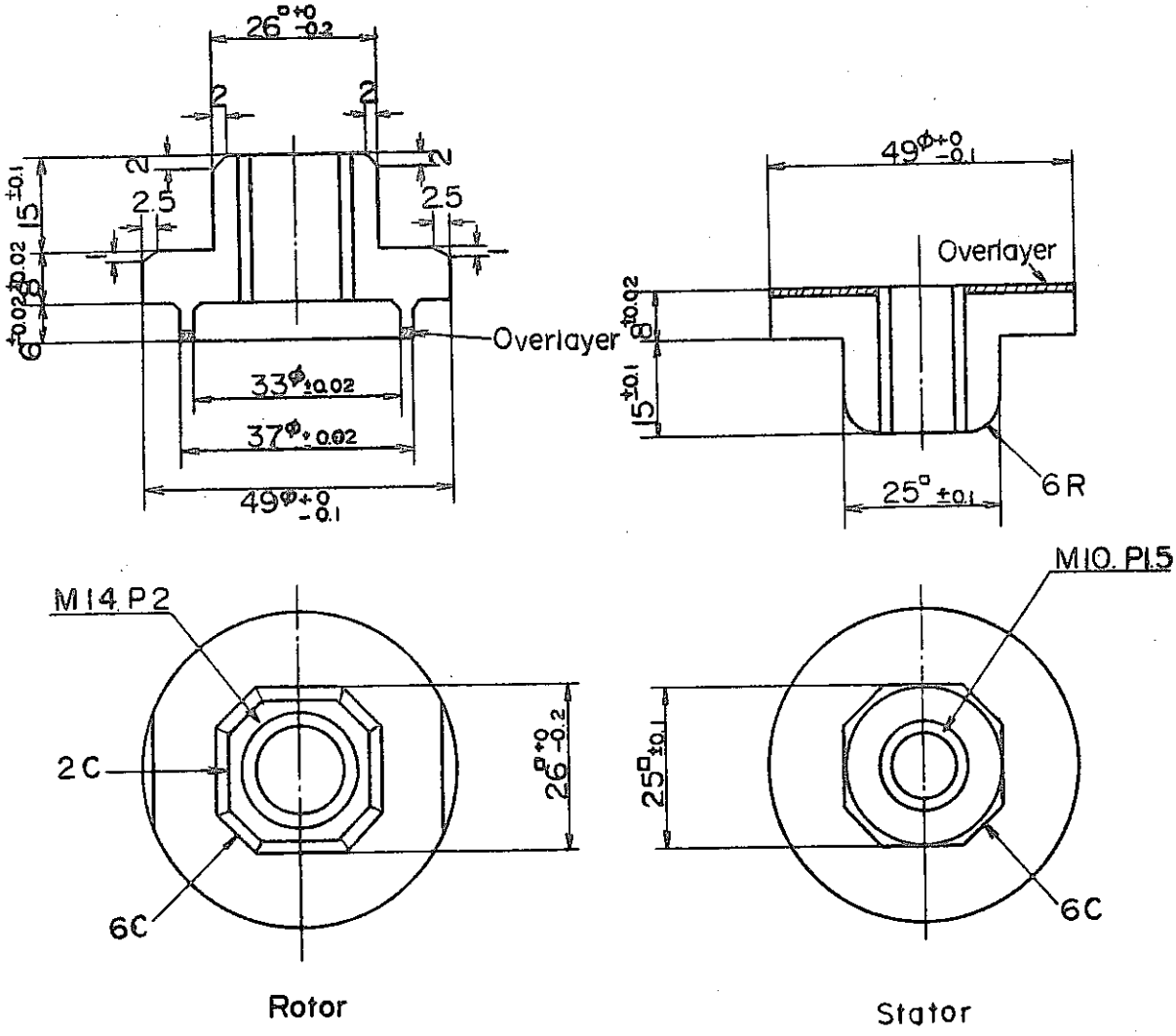

Fig. 3 Size of Test Piece

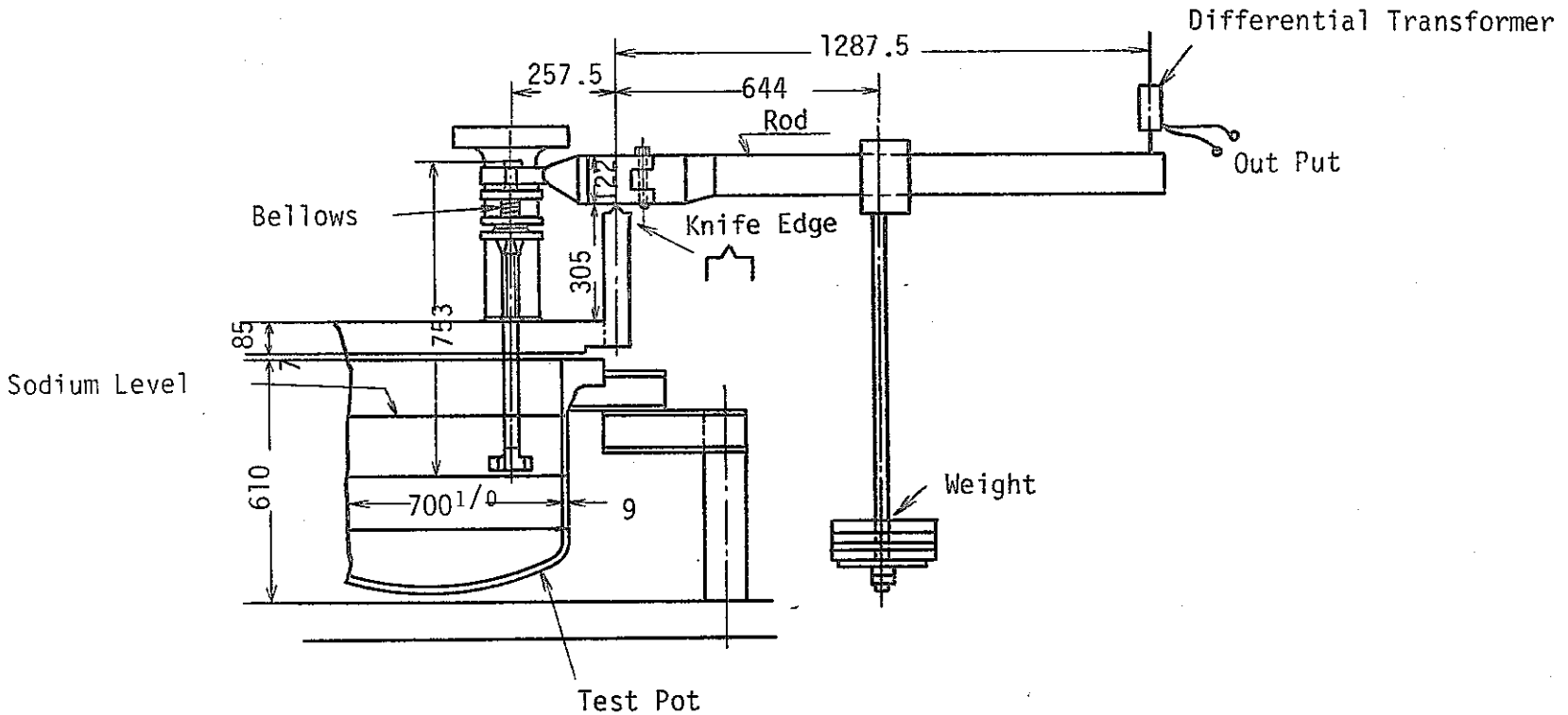

Fig. 4 Load Equipment

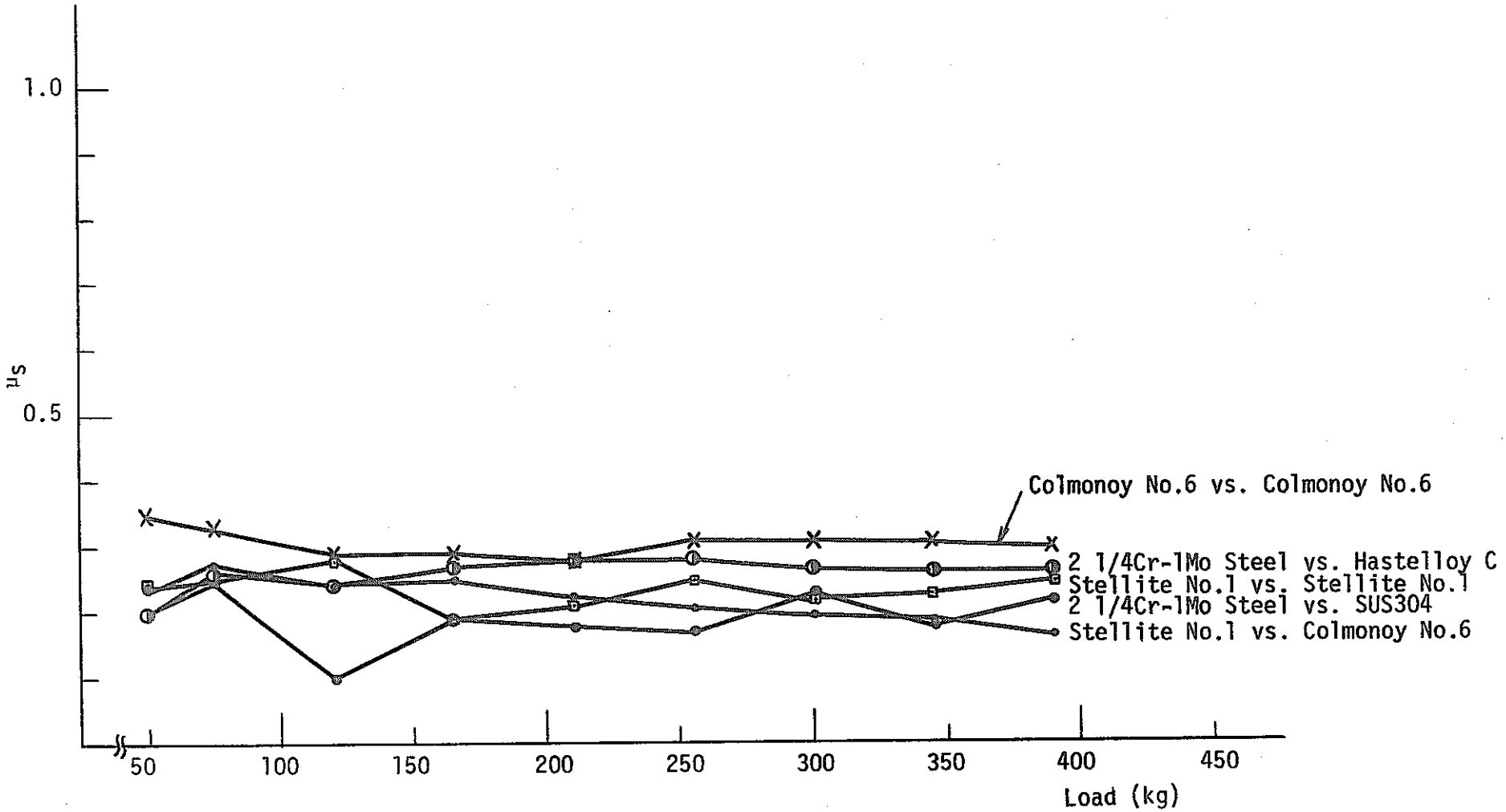

Fig. 5 μ_s vs. Load at 280°C

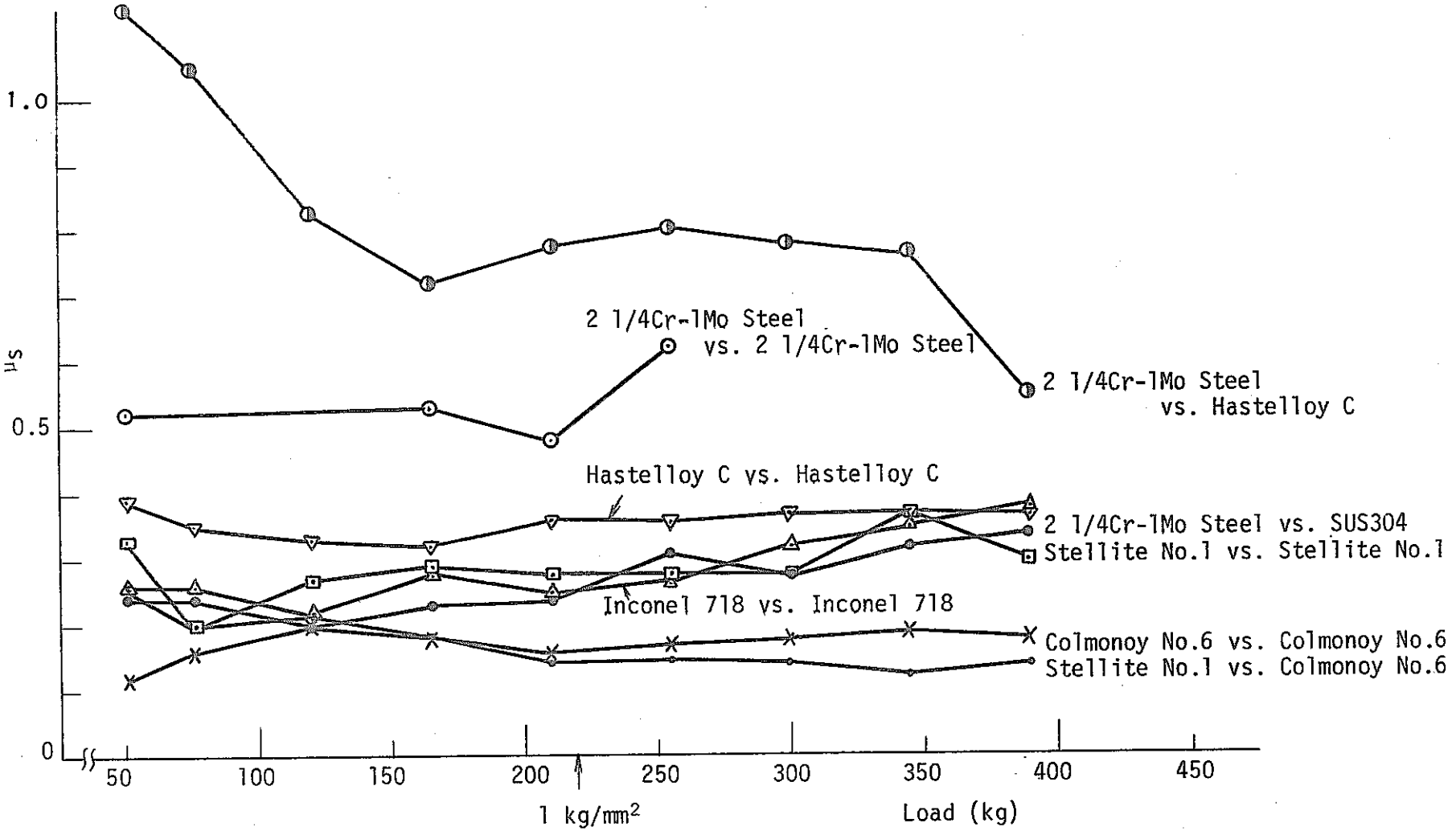

Fig. 6 μ_s vs. Load at 450°C

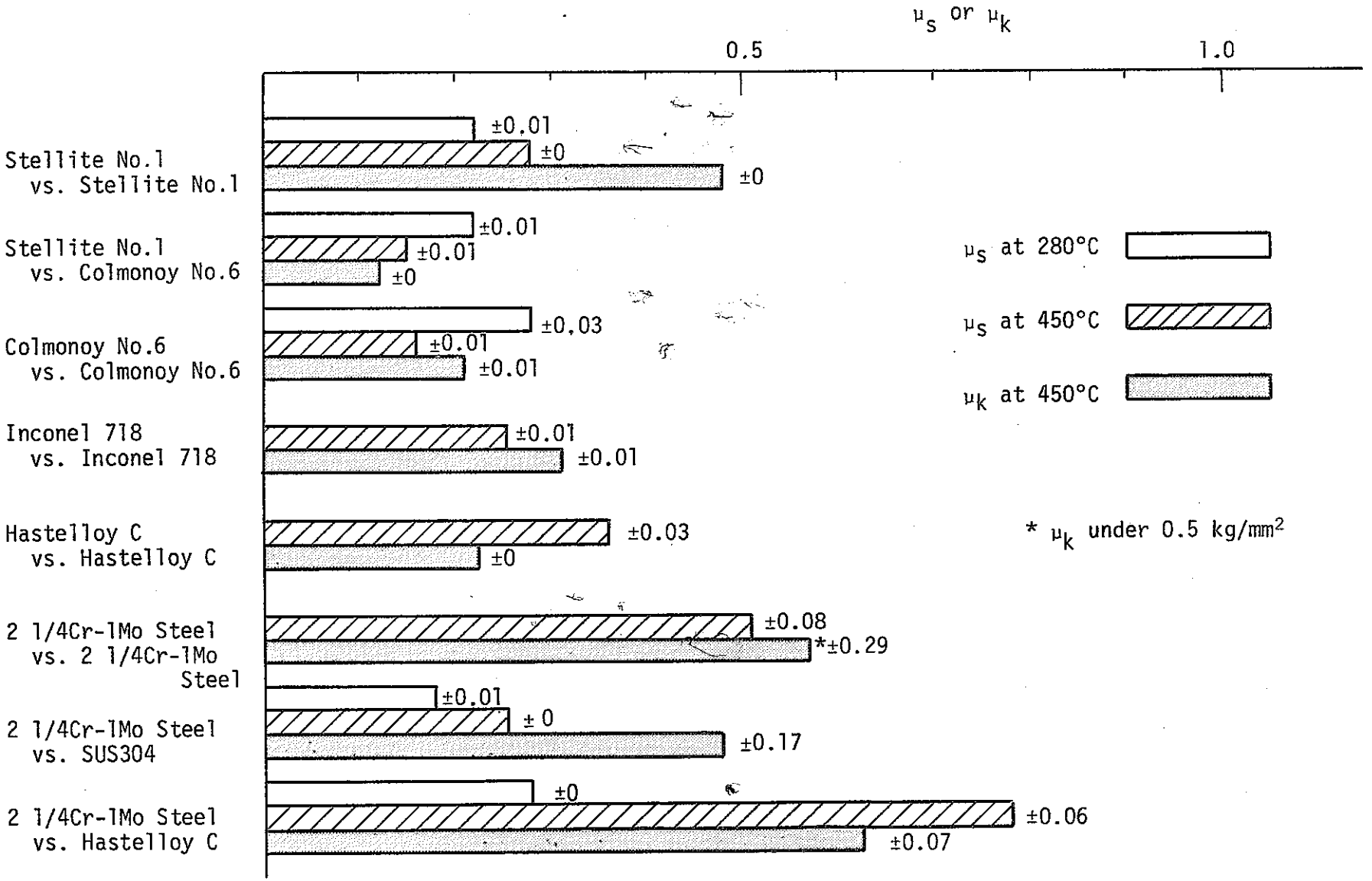

Fig. 7 μ_s and μ_k under 1 kg/mm²

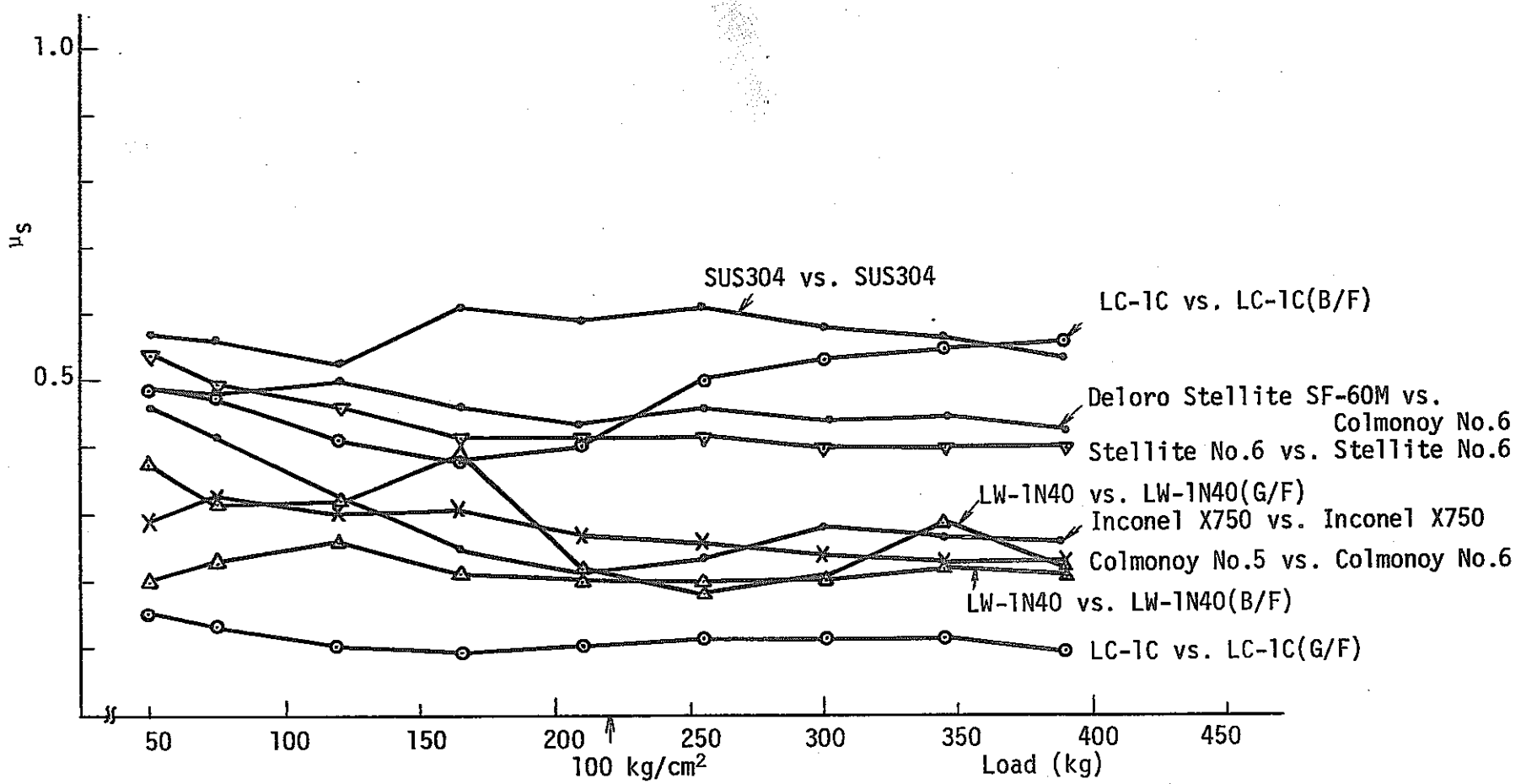

Fig. 8 s_n vs. Load (quoted from the Preceding Report[3])

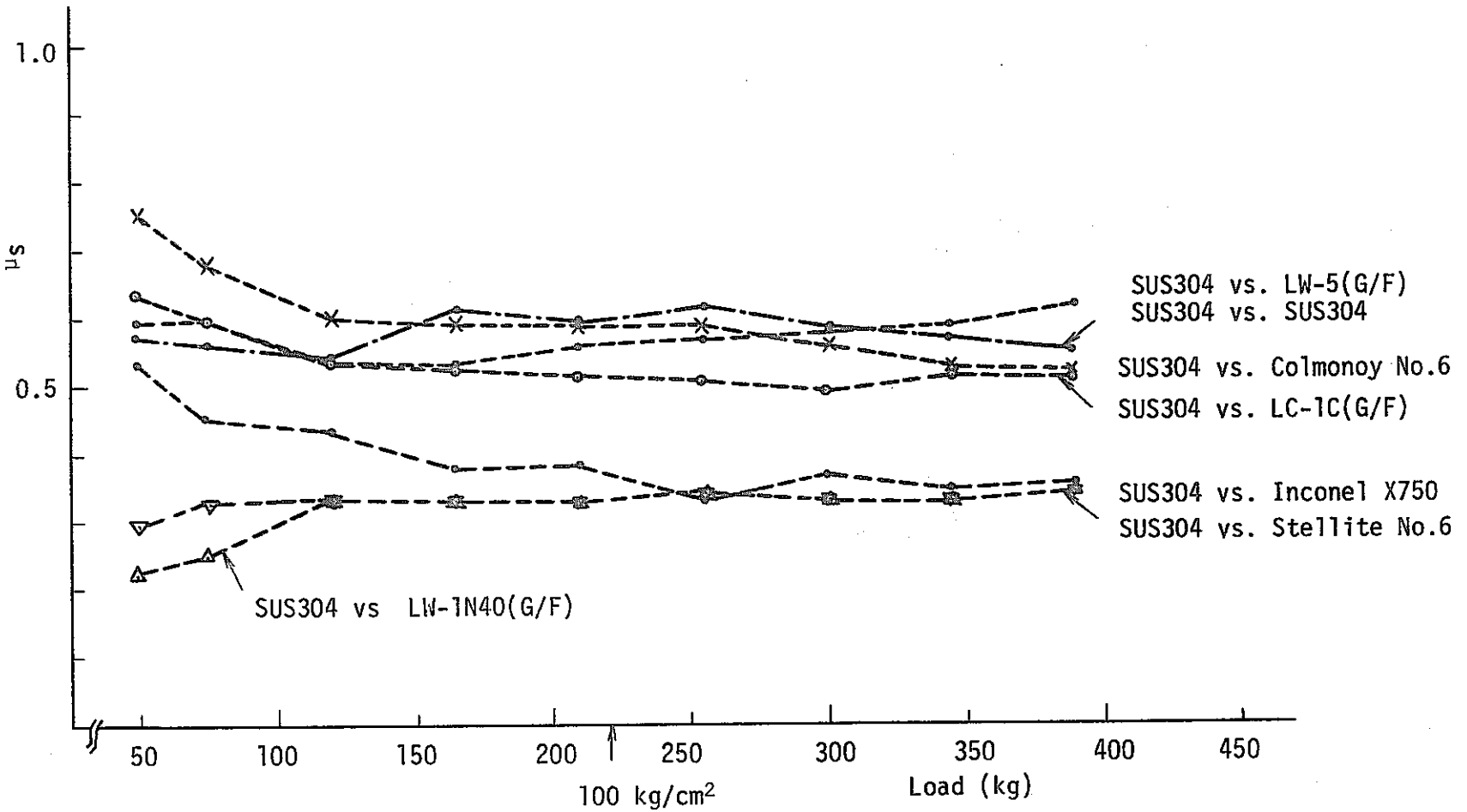

Fig. 9 s_H vs. Load (A Pair Coupled with SUS304) (quoted from the Preceding Report[3])

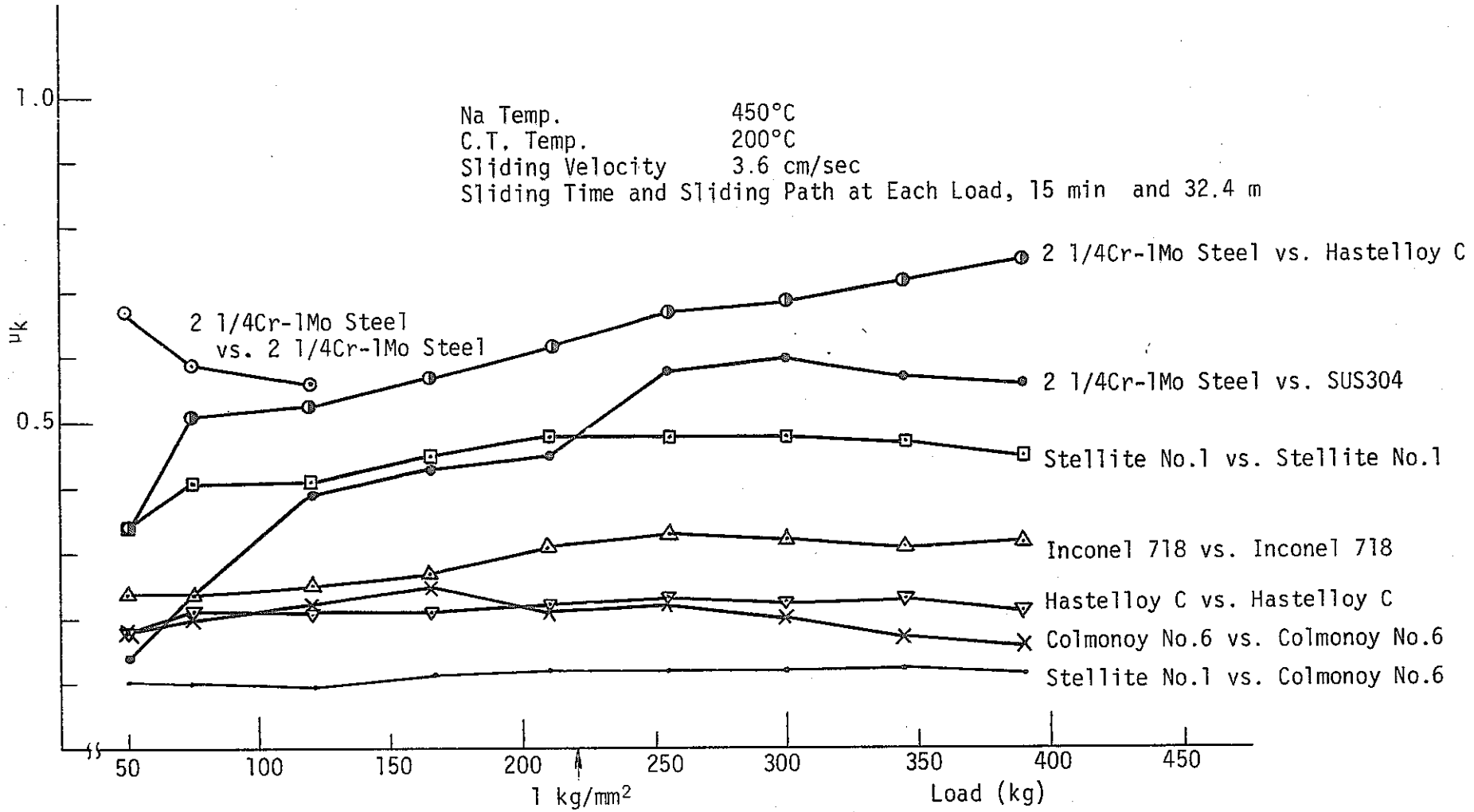

Fig. 10 μ_k vs. Load

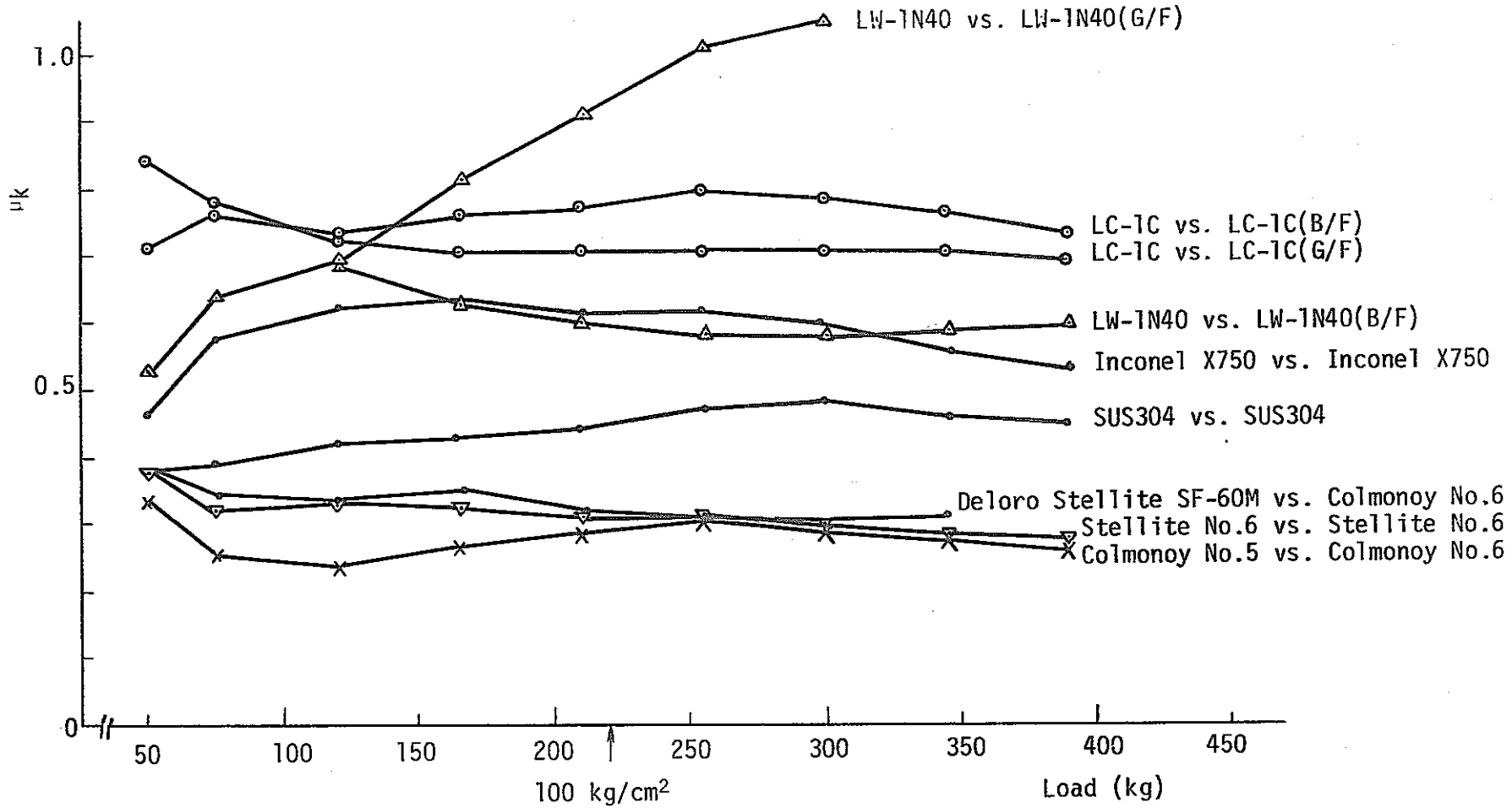

Fig. 11 μ_k vs. Load (quoted from the Preceding Report[3])

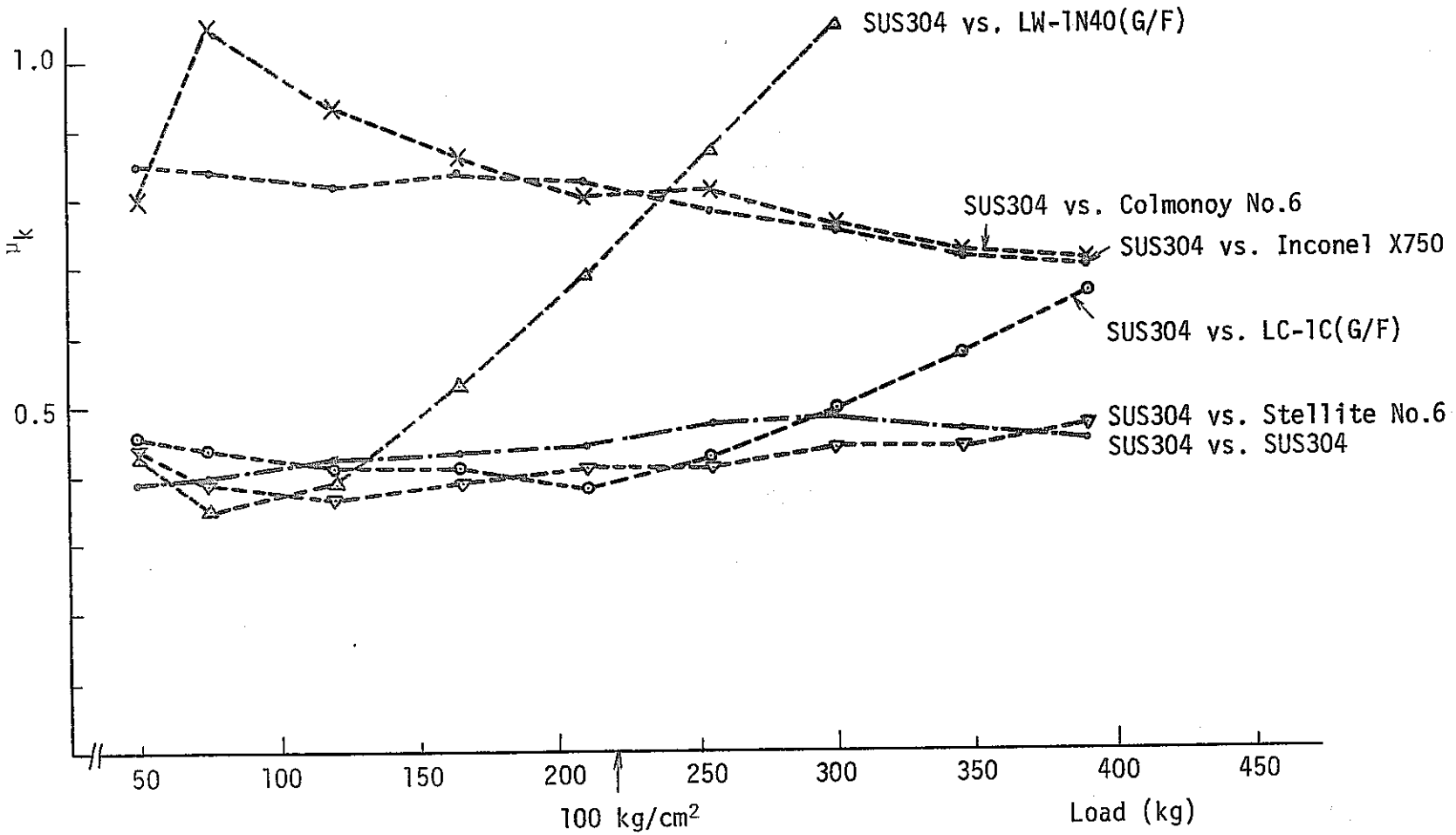

Fig. 12 k vs. Load (A Pair Coupled with SUS304) (quoted from the preceding Report[3])

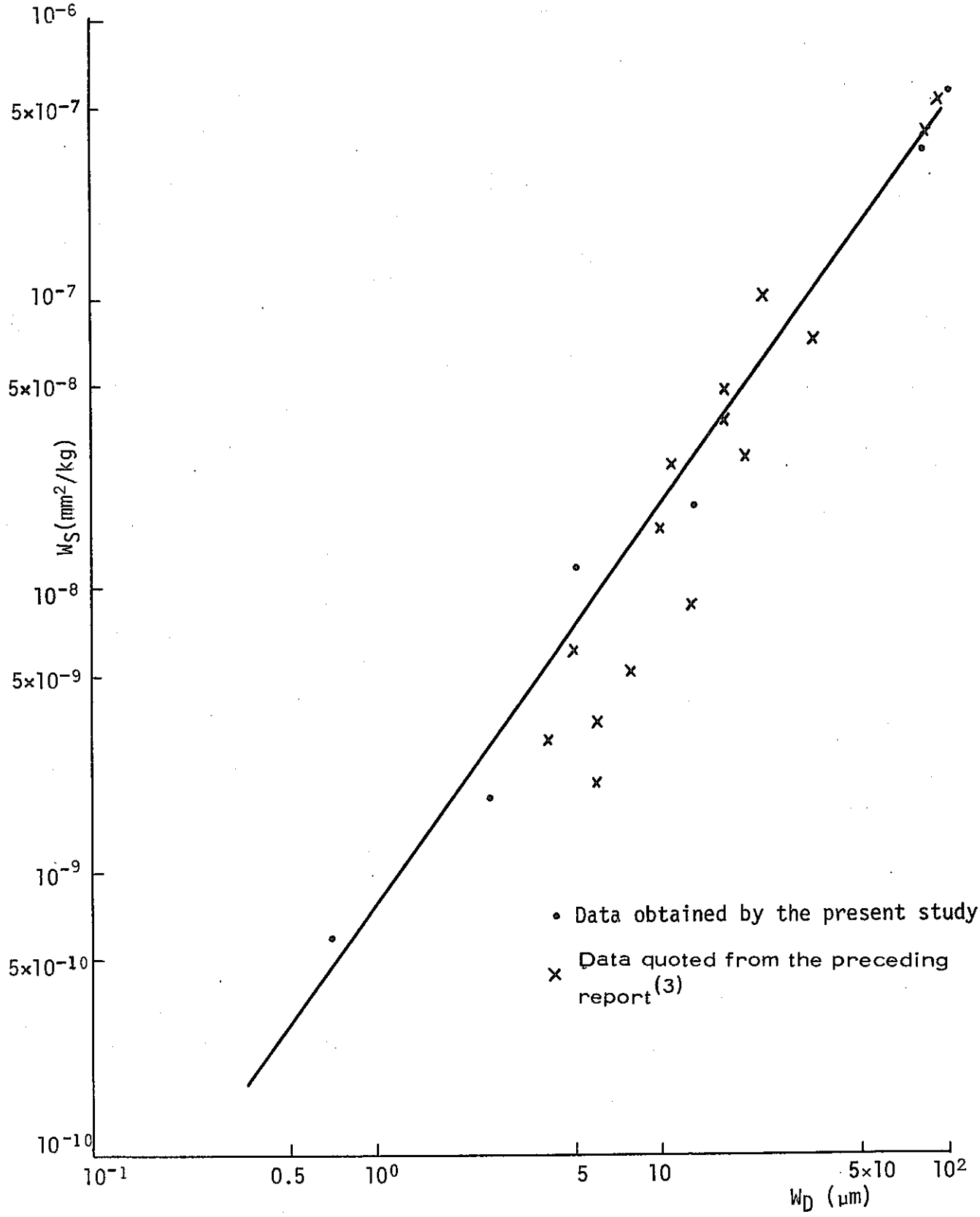

Fig. 13 W_S vs. W_D Relating to Stator

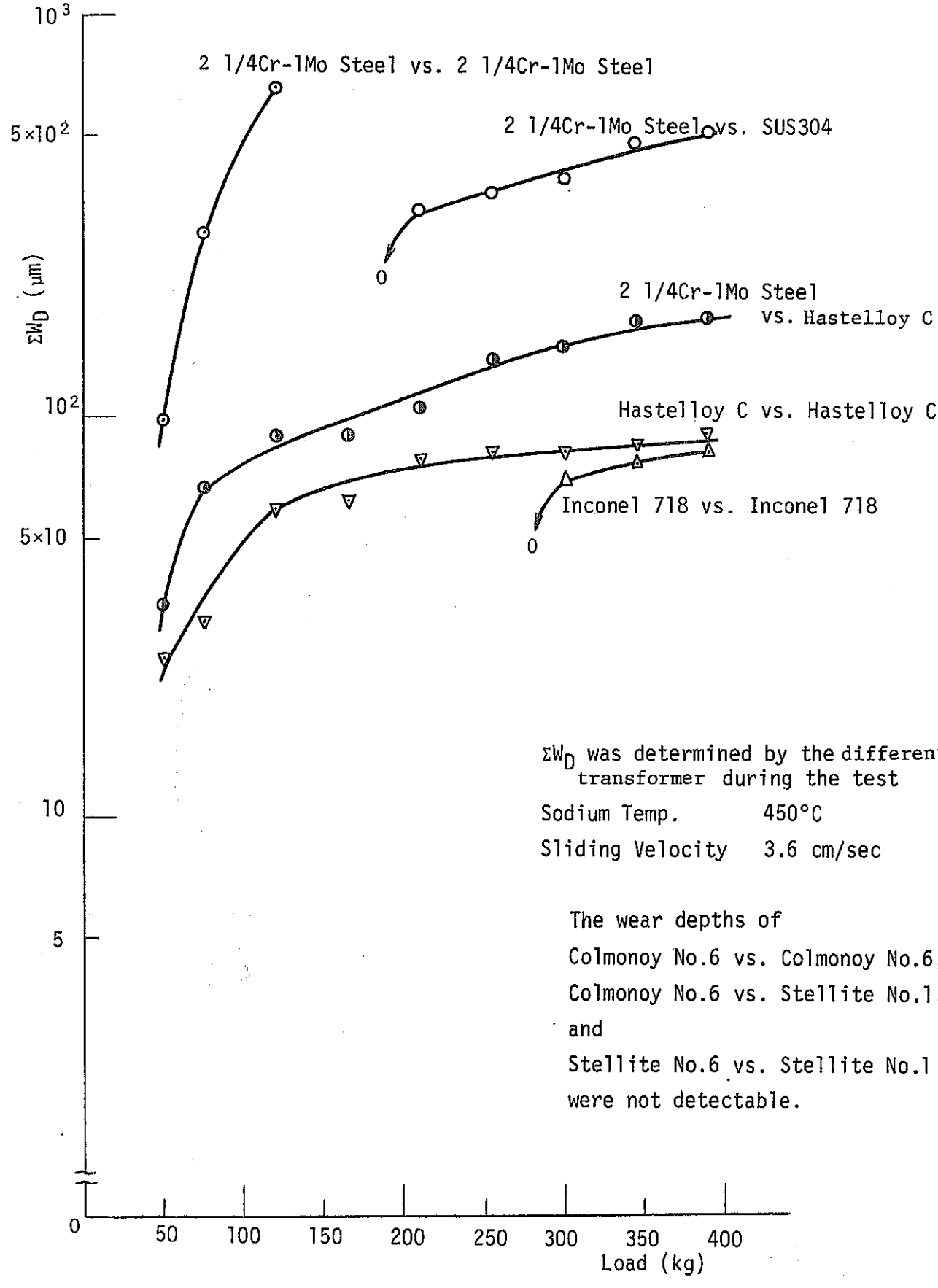

Fig. 14(A) ΣW_D vs. Load Relating to Materials Described in the Present Report.

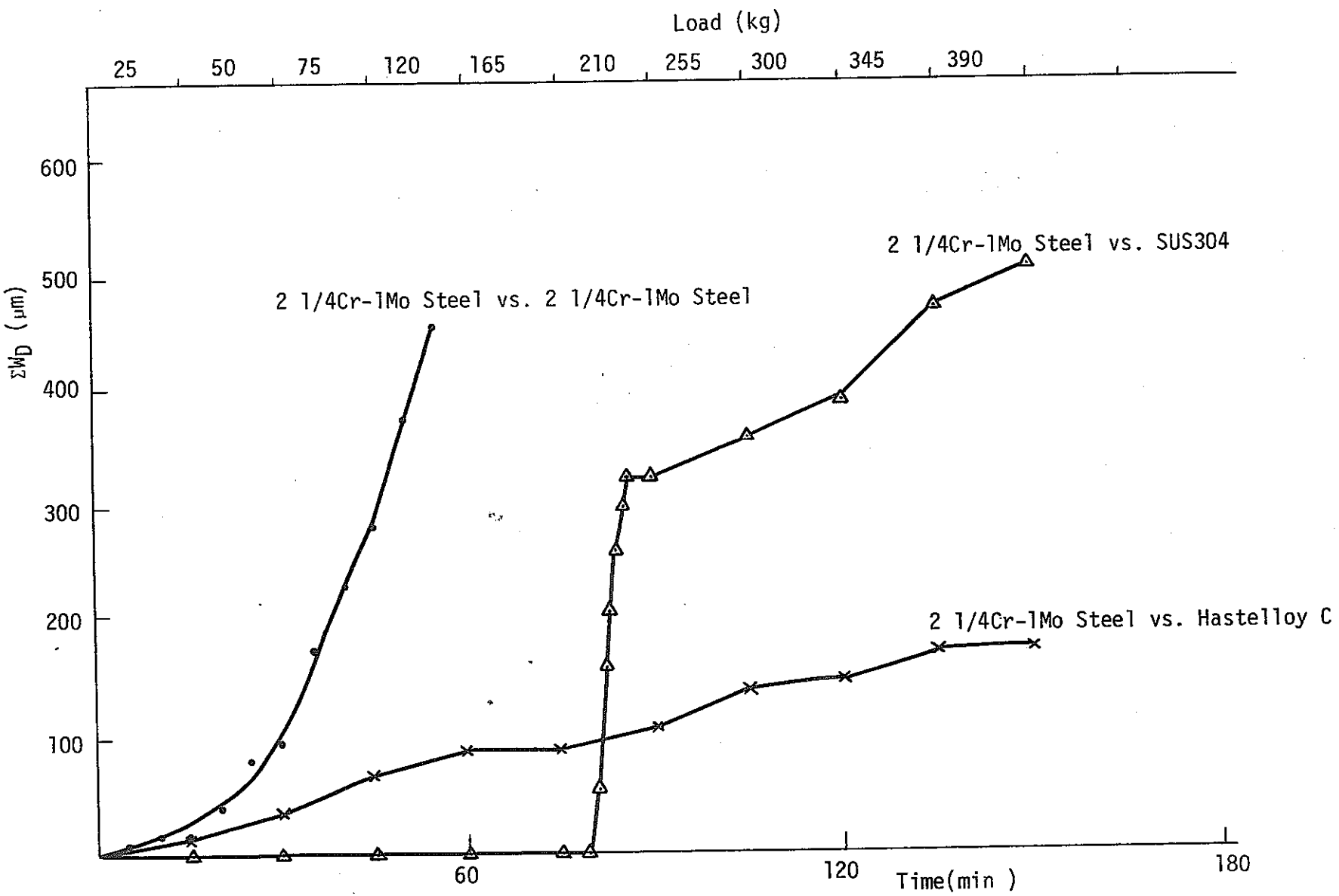

Fig. 14(B) ΣW_D vs. Time

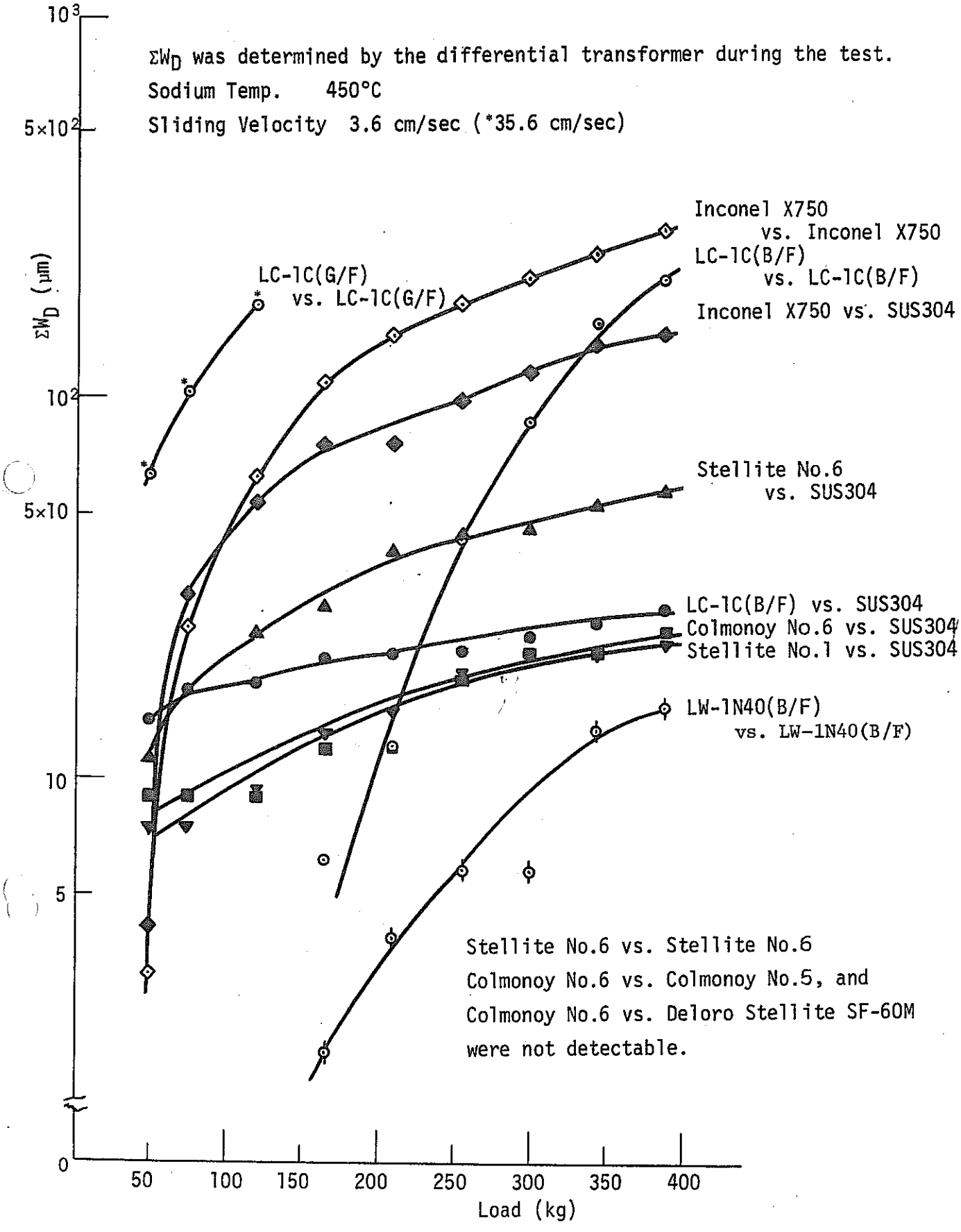

Fig. 15 ΣW_D vs. Load Relating to Materials Described in the Preceding Report[2],[3]

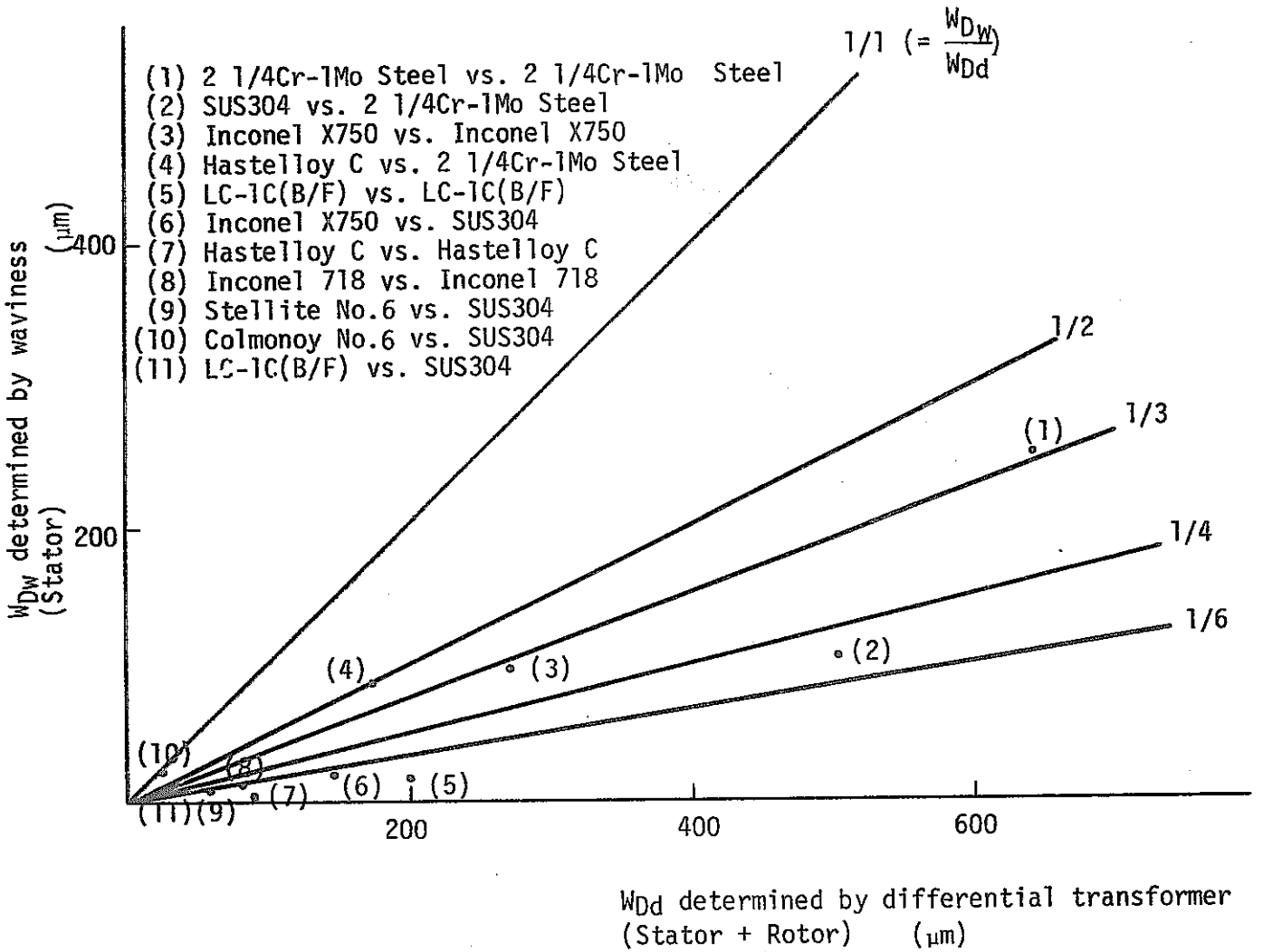

Fig. 16 Comparison of W_D Determined by Different Methods

Stellite No.1

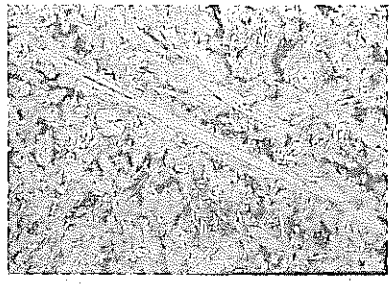

×100

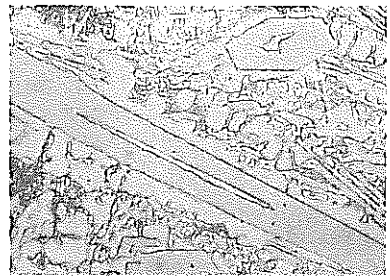

×400

Etched by Aqua Regia

Colmonoy No.6

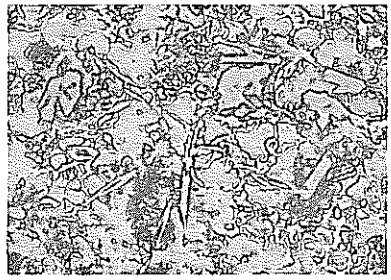

×100

Etched by Aqua Regia

Inconel 718

×100

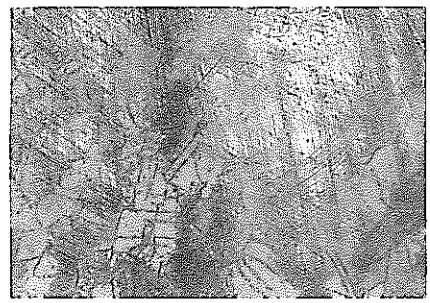

×200

Etched by $CuCl_2$+ Mixed Acid

Hastelloy C

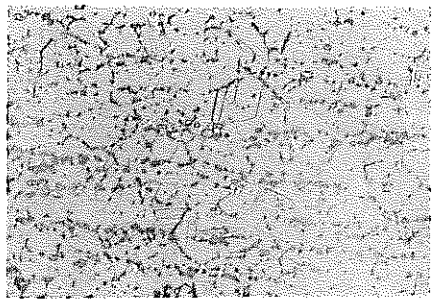

×100

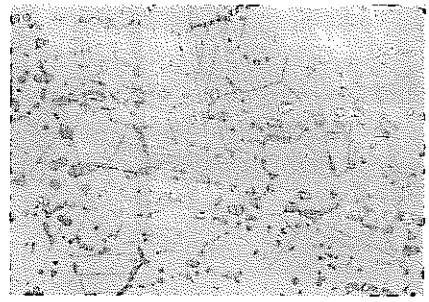

×200

Etched by $CuCl_2$+ Mixed Acid

2 1/4Cr-1Mo Steel

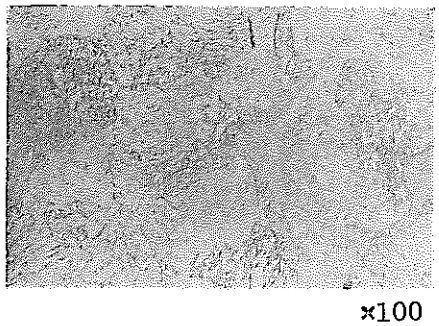

×100

×200

Etched by 10% Nital

Photo. 1 Cross-Sectional Micrographs of Test Pieces as Received

(A) vs. Stellite No.1

×100

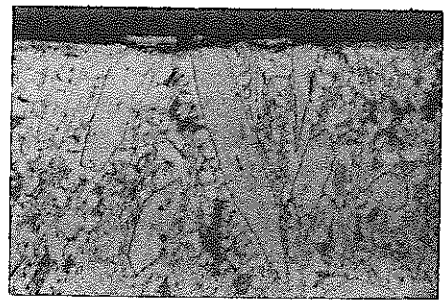

×200

(B) vs. Colmonoy No.6

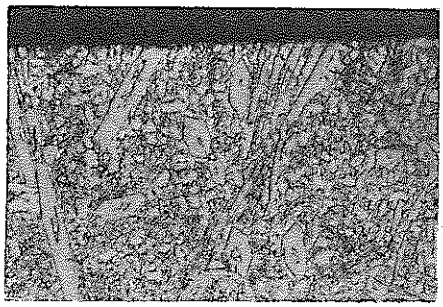

×100

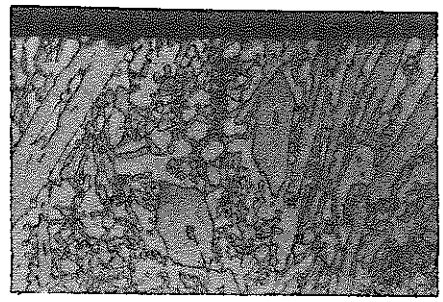

×200

3.6 cm/sec

max. 390 kg

Photo. 2 Cross-Sectional Micrographs of Stellite No. 1

(A) vs. Colmonoy No.6

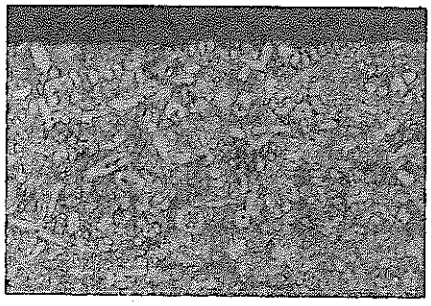

×100

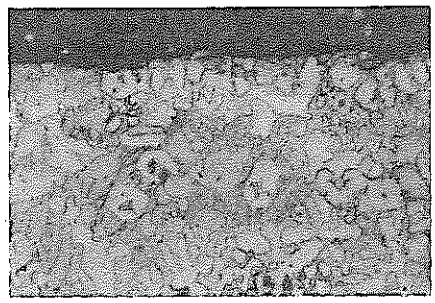

×200

(B) vs. Stellite No.1

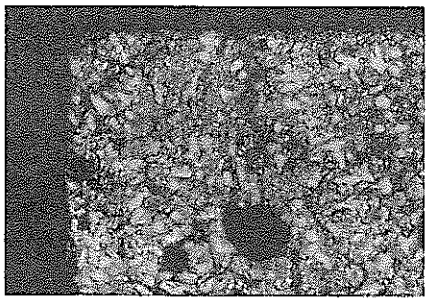

×100

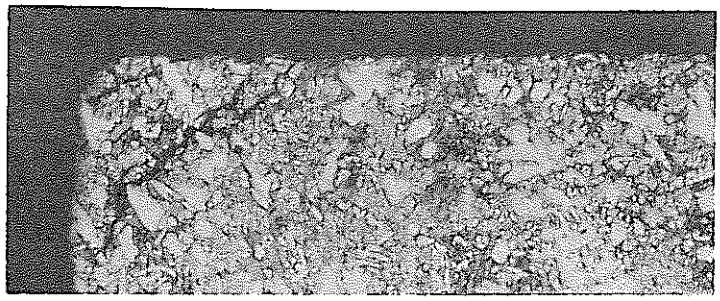

×200

3.6 cm/sec , max. 390 kg

Photo. 3 Cross-Sectional Micrographs of Colmonoy No.6

vs. Inconel 718, 3.6 cm/sec, max. 390 kg

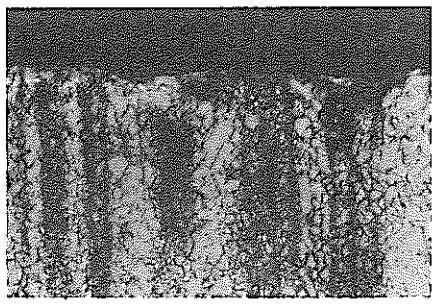

×100

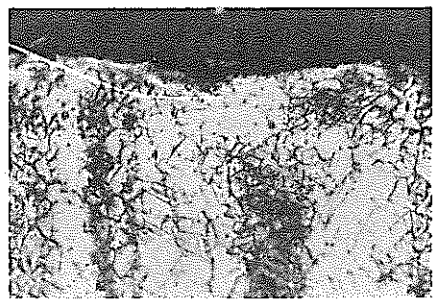

×200

Photo. 4 Cross-Sectional Micrographs of Inconel 718

(A) vs. Hastelloy C, 3.6 cm/sec, max. 390 kg

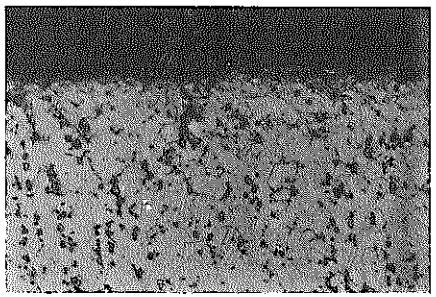

×100

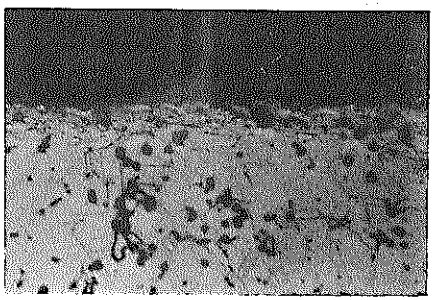

×200

(B) vs. 2 1/4Cr-1Mo Steel, 3.6 cm/sec, max. 390 kg

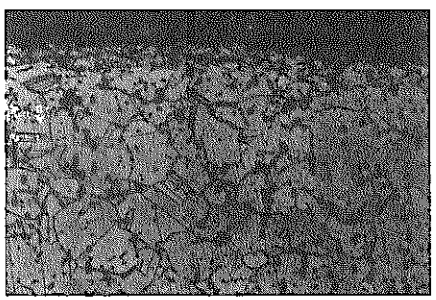

×100

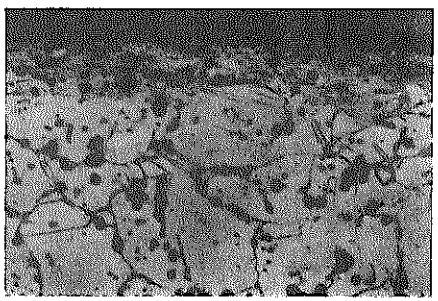

×200

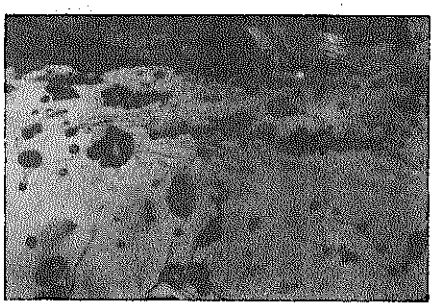

×400

Photo. 5 Cross-Sectional Micrographs of Hastelloy C

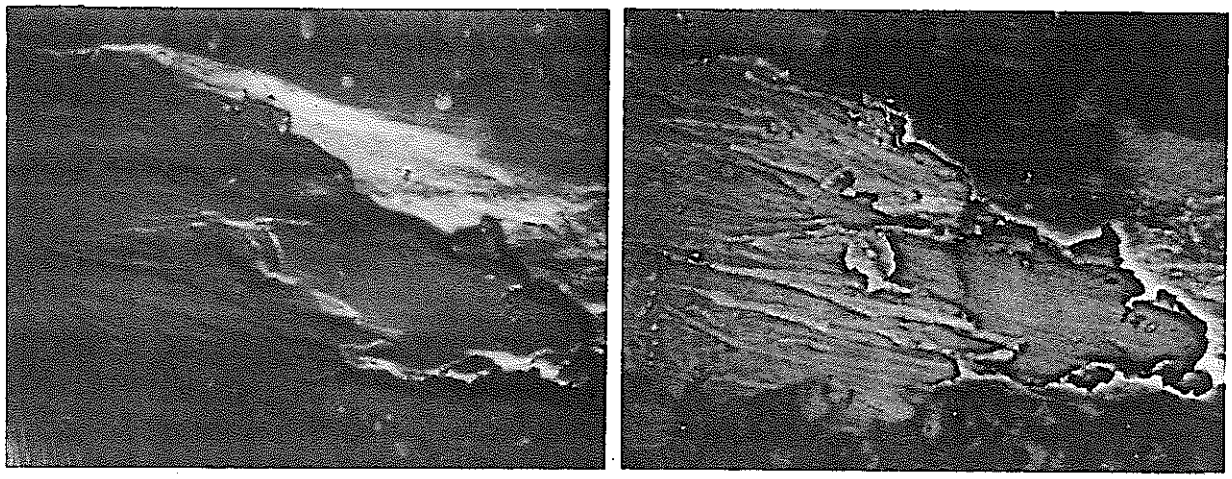

Sliding Surface to be Analyzed

Reflected Electron Image

Absorbed Electron Image

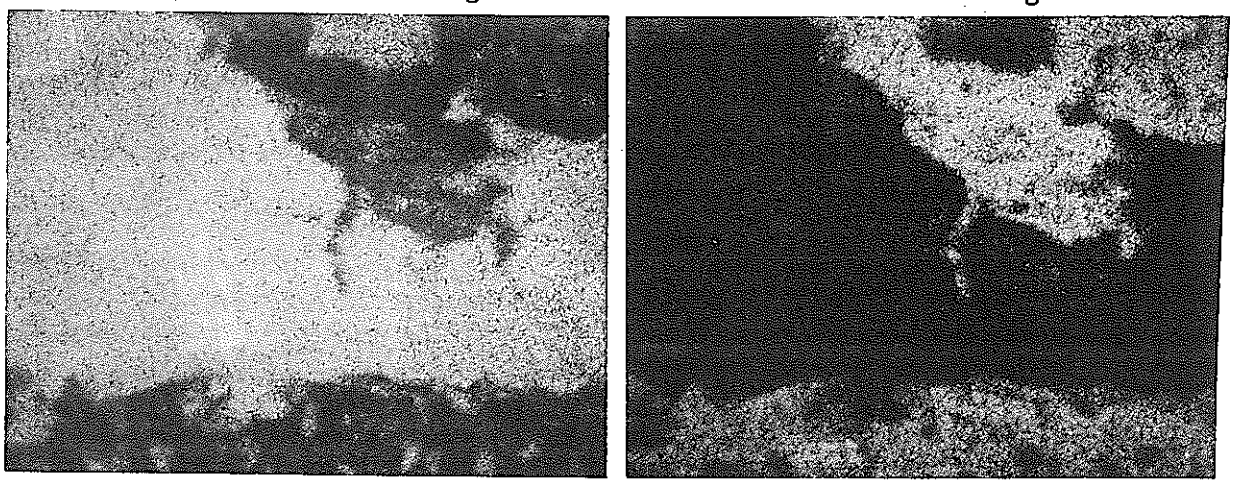

Fe

Ni

W

vs. 2 1/4Cr-1Mo Steel

150μm

Photo. 6 Electron Probe Microanalysis of Hastelloy C

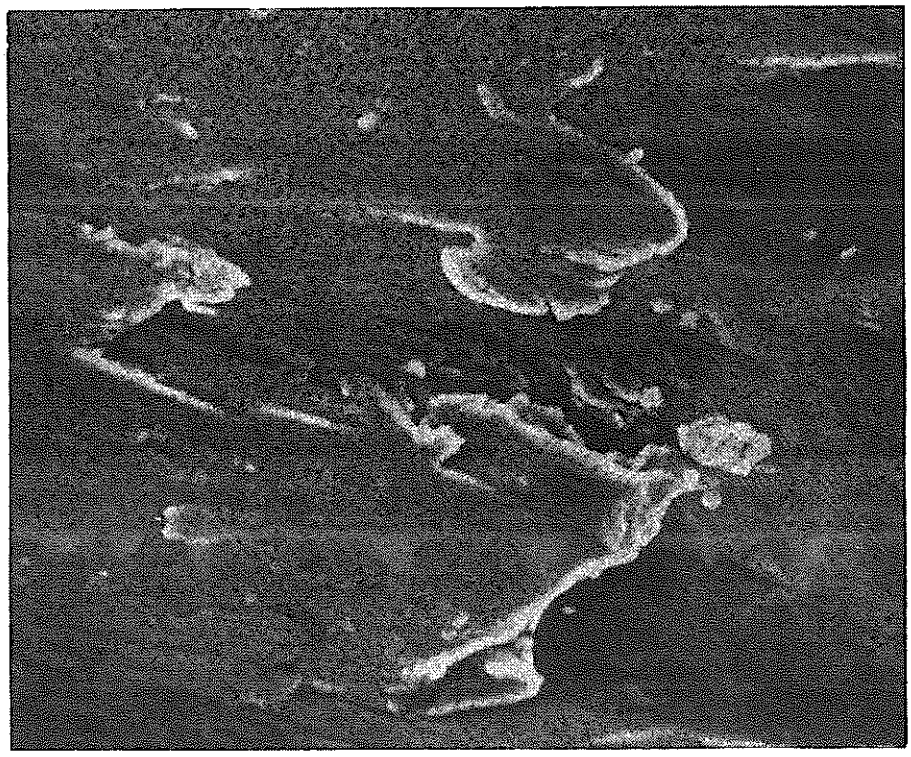

×1000

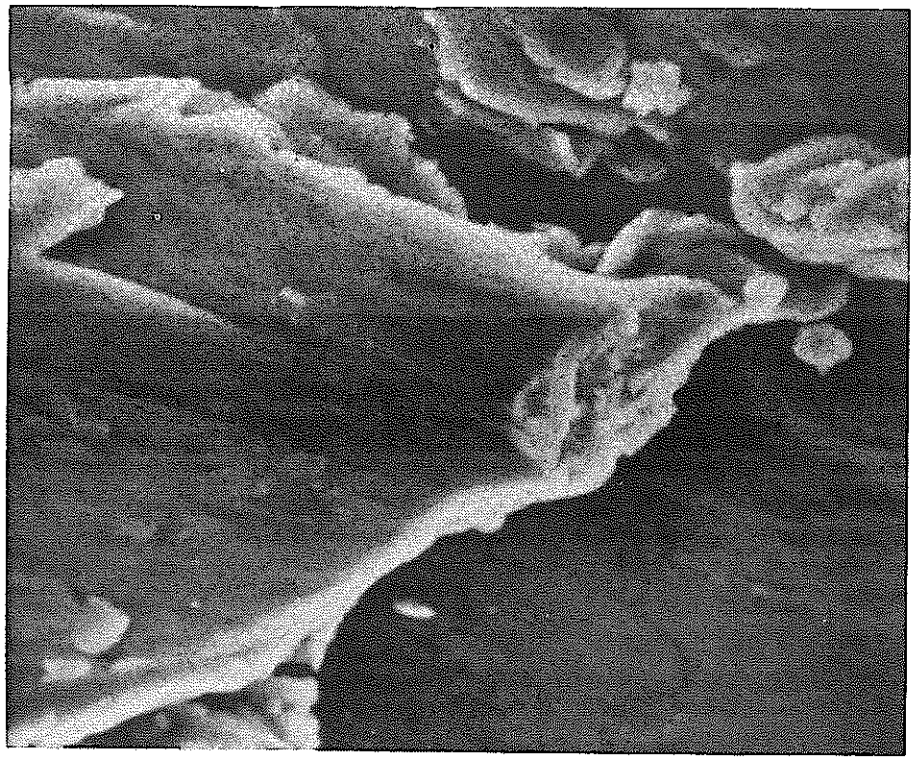

3.6 cm/sec

Max. 390 kg

vs. 2 1/4 Cr-1Mo Steel

×3000

Photo. 7 Scanning Electron Probe Microscopy of Hastelloy C

(A) vs. 2 1/4Cr-1Mo Steel, 3.6 cm/sec, max. 390 kg

×50

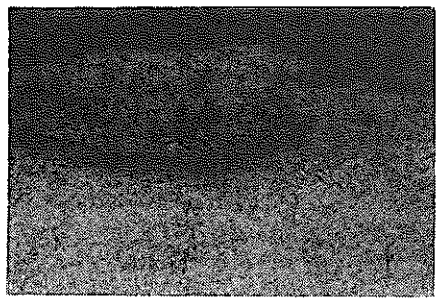

×100

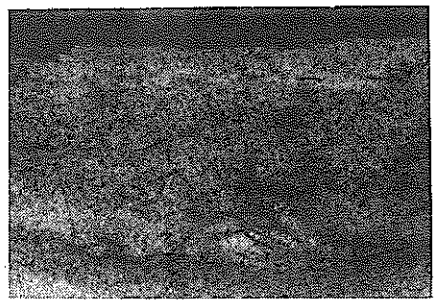

×200

(B) vs. SUS 304, 3.6 cm/sec, max. 390 kg

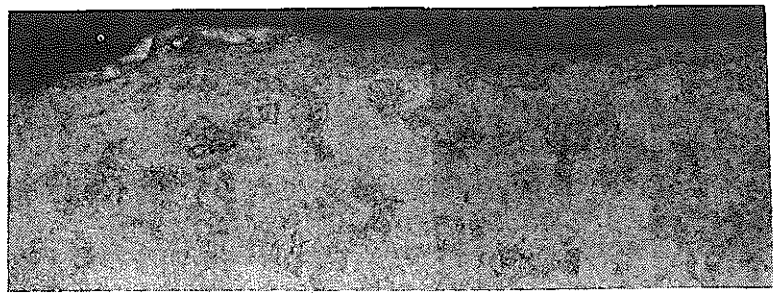

×50

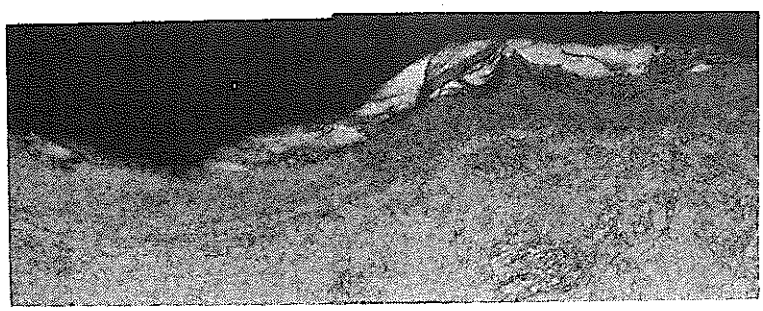

×100

×200

(C) vs. Hastelloy C, 3.6 cm/sec, max. 390 kg

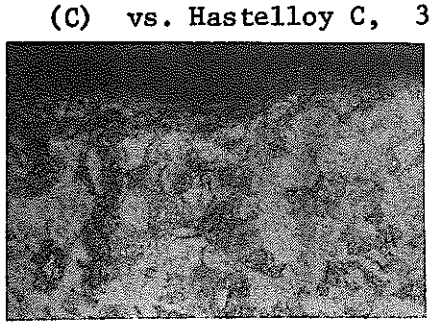

×50

×100

×200

Photo. 8 Cross-Sectional Micrographs of 2 1/4 Cr-1Mo Steel

vs. 2 1/4Cr-1Mo Steel, 3.6 cm/sec, max. 390 kg

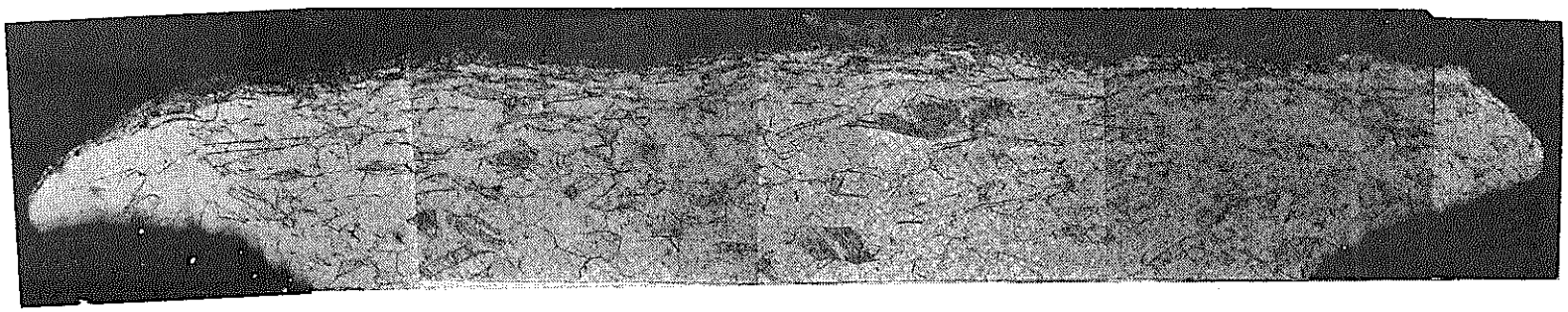

×50, Etched with Aqua Regia

×200, Etched with 10% Nital

Photo. 9 Cross-Sectional Micrographs of SUS 304

(A) as Received


×500

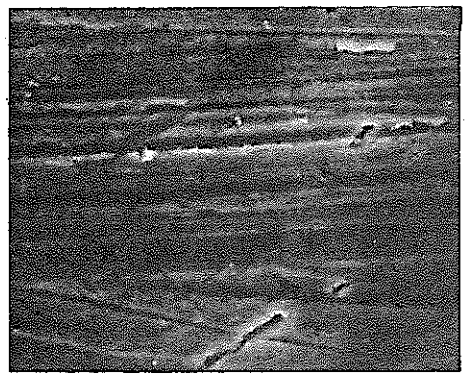
×1500

(B) vs. 2 1/4Cr-1Mo Steel, 3.6 cm/sec, max. 390 kg

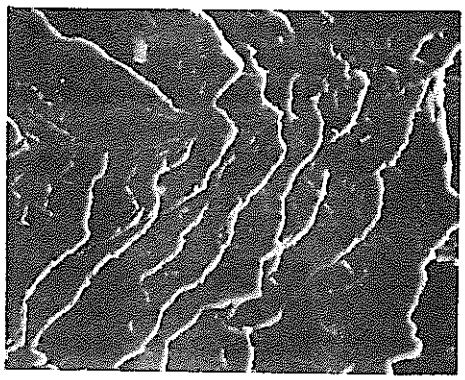
×500

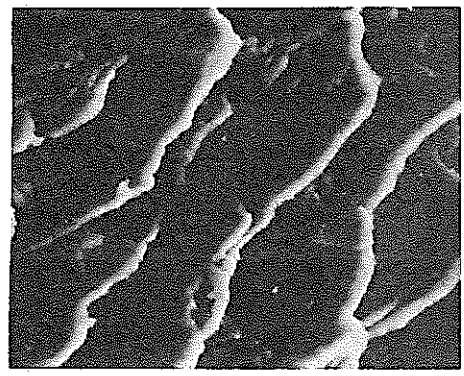
×1500

(C) vs. SUS 304, 3.6 cm/sec, max. 390 kg

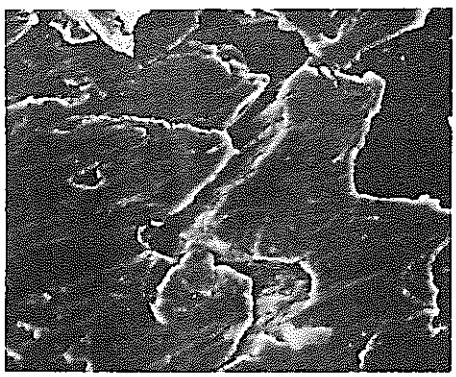
×500

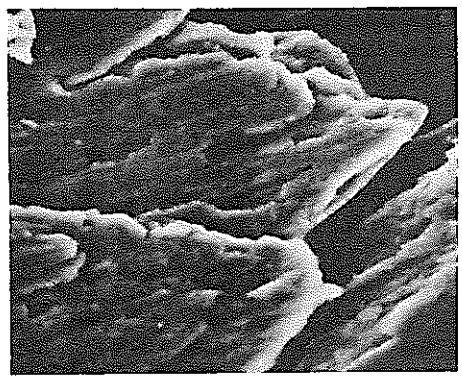
×1500

(D) vs. Hastelloy C, 3.6 cm/sec, max. 390 kg

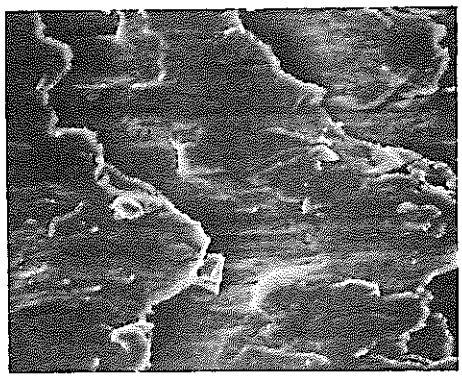
×500


×1500

Photo. 10 Scanning Electron Probe Microscopy of 2 1/4Cr-1Mo Steel

vs. 2 1/4Cr-1Mo Steel, 3.6 cm/sec, max. 390 kg

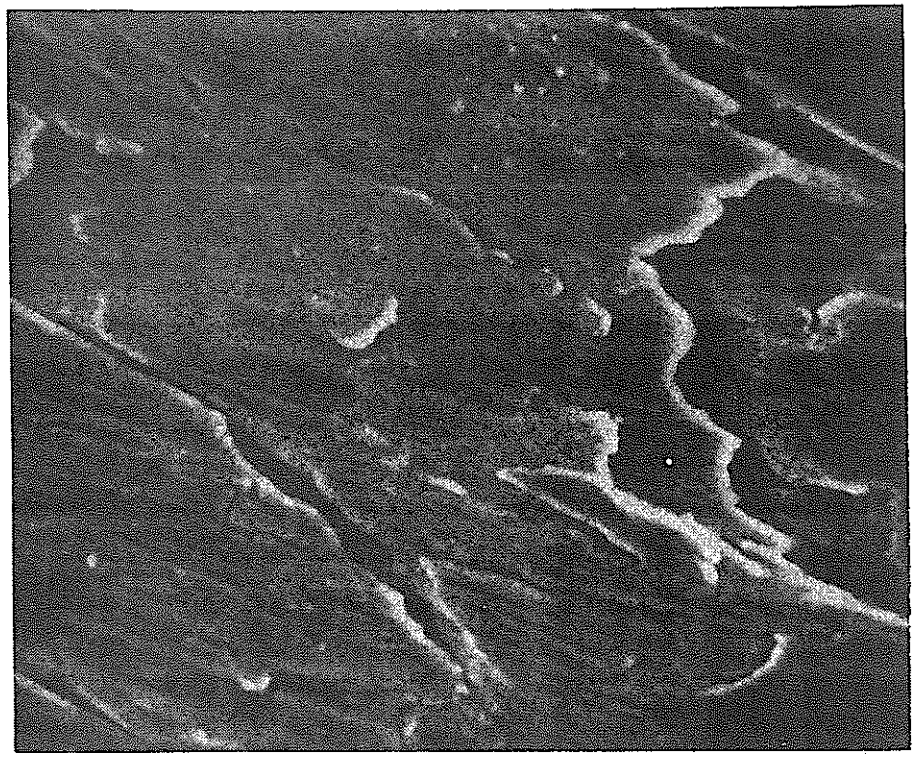

×1000

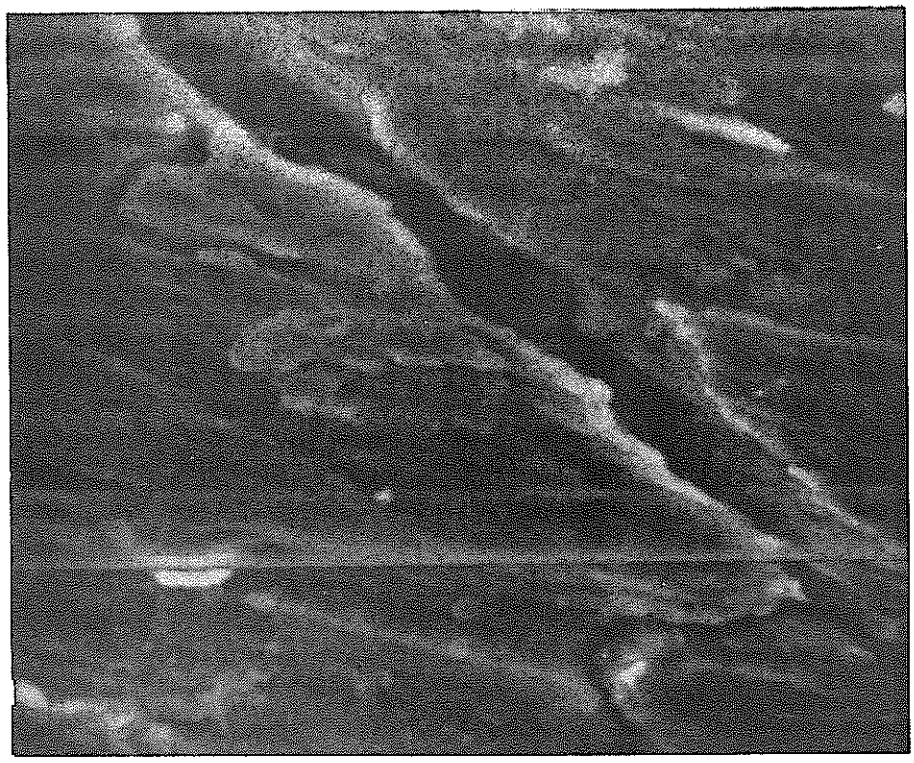

×3000

Photo. 11 Scanning Electron Probe Microscopy of SUS 304

(A) vs. SUS 304, 3.6 cm/sec, max. 390 kg

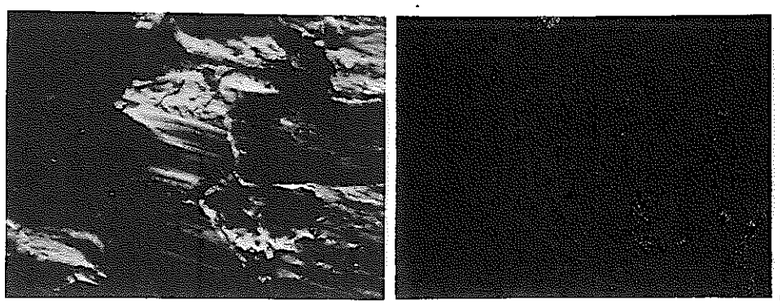

Sliding Surface to be Analyzed

Ni

(B) vs. SUS 304, 3.6 cm/sec, max. 390 kg

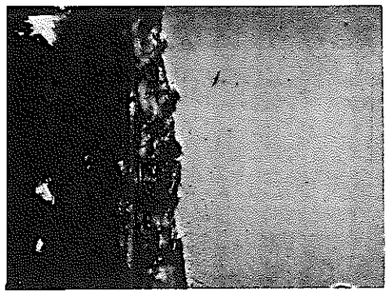

Sliding Cross-Section to be Analyzed

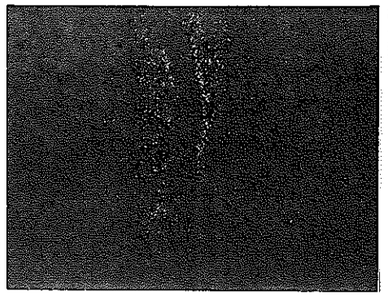

Ni

(C) vs. Hastelloy C, 3.6 cm/sec, max. 390 kg

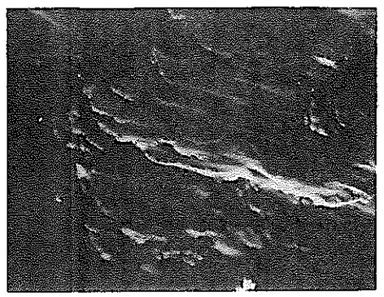

Sliding Surface to be Analyzed

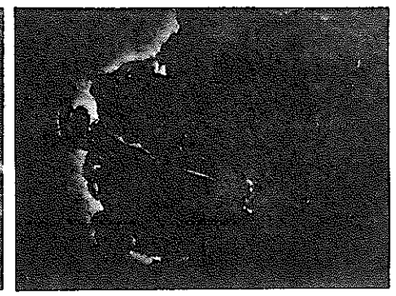

Reflected Electron Image

Absorbed Electron Image

Cr

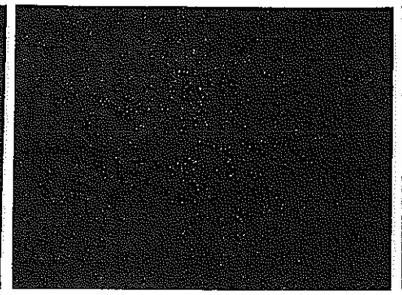

Mo

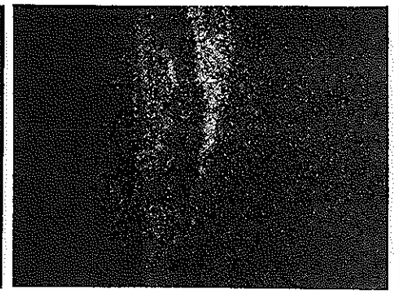

Cr

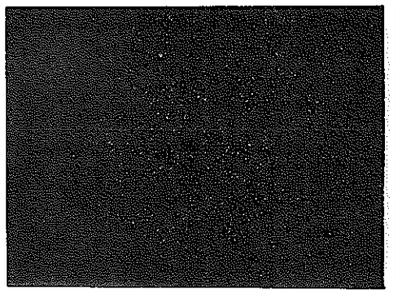

Mo

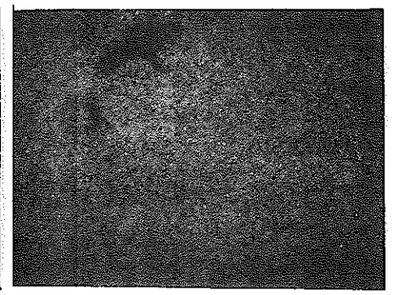

Fe

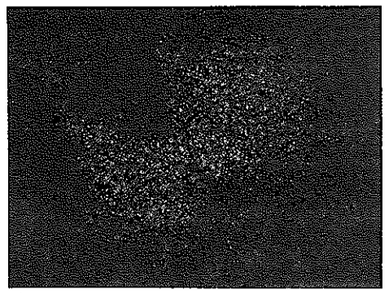

Ni

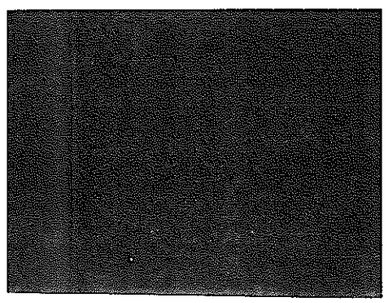

150μm

Photo. 12 Electron Probe Microanalysis of 2 1/4Cr-1Mo Steel

Sliding Surface to be Analyzed

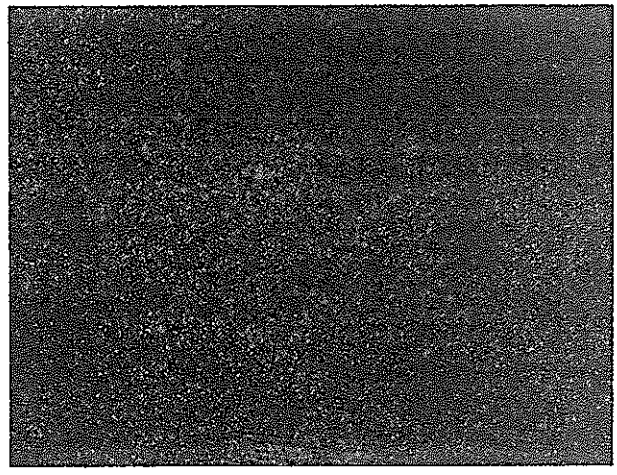

Ni

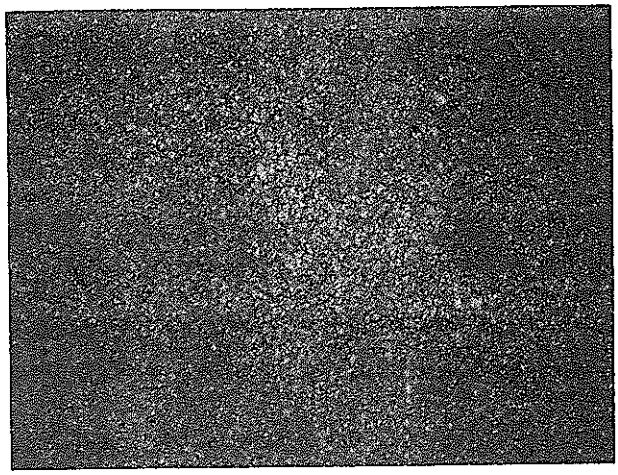

Cr

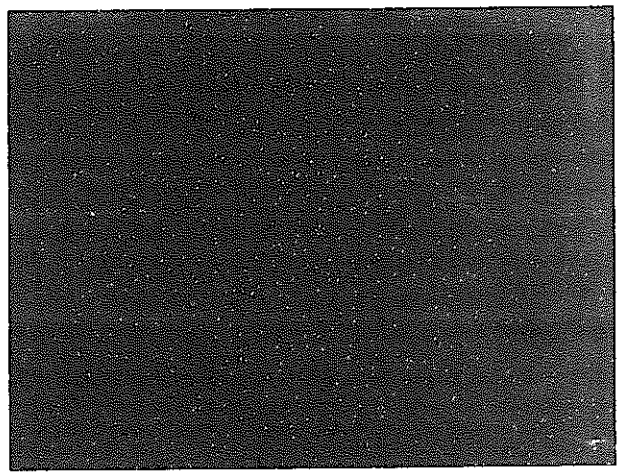

Mo

150μm

vs. 2 1/4Cr-1Mo Steel, 3.6 cm/sec

max. 390 kg

Photo. 13 Electron Probe Microanalysis of SUS 304